

Leverage-Weighted Conformal Prediction

Shreyas Fadnavis¹

¹shreyasfadnavis@gmail.com

Abstract

Split conformal prediction provides distribution-free prediction intervals with finite-sample marginal coverage, but produces constant-width intervals that overcover in low-variance regions and undercover in high-variance regions. Existing adaptive methods require training auxiliary models. We propose Leverage-Weighted Conformal Prediction (LWCP), which weights nonconformity scores by a function of the statistical leverage—the diagonal of the hat matrix—deriving adaptivity from the geometry of the design matrix rather than from auxiliary model fitting. We prove that LWCP preserves finite-sample marginal validity for any weight function; achieves asymptotically optimal conditional coverage at essentially no width cost when heteroscedasticity factors through leverage; and recovers the form and width of classical prediction intervals under Gaussian assumptions while retaining distribution-free guarantees. We further establish that randomized leverage approximations preserve coverage exactly with controlled width perturbation, and that vanilla CP suffers a persistent, sample-size-independent conditional coverage gap that LWCP eliminates. The method requires no hyperparameters beyond the choice of weight function and adds negligible computational overhead to vanilla CP. Experiments on synthetic and real data confirm the theoretical predictions, demonstrating substantial reductions in conditional coverage disparity across settings.

1 INTRODUCTION

Conformal prediction (CP) has become the dominant paradigm for distribution-free uncertainty quantification (Shafer and Vovk, 2008, Vovk et al., 2005). In regression,

split conformal prediction (Lei et al., 2018, Papadopoulos et al., 2002) produces intervals $\hat{\mathcal{C}}_n(x) = \hat{f}(x) \pm \hat{q}$, where \hat{q} is an empirical quantile of calibration residuals. While guaranteeing marginal coverage $\mathbb{P}(Y_{n+1} \in \hat{\mathcal{C}}_n(X_{n+1})) \geq 1-\alpha$, these intervals have *constant width*—a well-documented limitation (Lei et al., 2018, Romano et al., 2019, Tibshirani, 2023)—and thus overcover in low-variance regions while undercovering in high-variance regions.

Existing adaptive methods address this by training auxiliary models: conformalized quantile regression (CQR; Romano et al., 2019) fits quantile regressors; studentized residual methods (Lei et al., 2018, Papadopoulos et al., 2008) fit a variance estimator $\hat{\sigma}(x)$; more recent approaches use Bayesian processes (Cabezas et al., 2025) or random forests (Amoukou and Brunel, 2023). All require additional hyperparameters, risk overfitting, and incur non-trivial computational overhead.

We propose a fundamentally different strategy: deriving the normalizer from the *geometry of the design matrix* using **statistical leverage scores**—the diagonal of the hat matrix $\mathbf{H} = \mathbf{X}(\mathbf{X}^\top \mathbf{X})^{-1} \mathbf{X}^\top$. Leverage scores quantify how far each point lies from the feature distribution centroid and directly govern prediction variance (Chatterjee and Hadi, 1986, Hoaglin and Welsch, 1978). They provide a closed-form, model-free weighting function for conformal scores that requires no auxiliary model fitting.

Contributions.

1. **Framework (Section 2).** We weight nonconformity scores by a function of leverage, yielding prediction intervals of width $2\hat{q}/w(h(x))$ that adapt to the geometry of the design matrix.
2. **Finite-sample coverage (Theorem 3.1).** LWCP preserves marginal validity ($\geq 1-\alpha$, tight to $O(1/n_2)$) for *any* weight function, as a direct consequence of exchangeability.
3. **Efficiency (Theorems 3.4 and 3.5).** Under a linear model with leverage-dependent heteroscedastic-

ity, the variance-stabilized weight $w^*(h) = 1/\sqrt{g(h)}$ achieves asymptotically optimal conditional coverage at negligible width cost (deviation controlled by $\rho^2 = \text{CV}^2(\sqrt{g(H)})$).

4. **Classical recovery (Theorem 3.9).** Under Gaussian assumptions, LWCP recovers the form and asymptotic width of classical prediction intervals while retaining distribution-free validity.
5. **Approximate leverage (Theorem 3.10).** Randomized SVD approximations preserve coverage exactly with controlled width perturbation, enabling $O(np \log p)$ computation.

1.1 RELATED WORK

Conformal prediction. Split conformal prediction (Lei et al., 2018, Papadopoulos et al., 2002, Vovk et al., 2005) guarantees marginal coverage but produces constant-width intervals. Distribution-free conditional coverage is impossible in general (Barber et al., 2021b, Vovk, 2012); see Tibshirani (2023) for a survey.

Adaptive and localized methods. Normalized nonconformity scores (Papadopoulos et al., 2008) and CQR (Romano et al., 2019) achieve adaptivity through auxiliary models. Jackknife+ (Barber et al., 2021a) provides $1-2\alpha$ coverage without splitting; localized CP (Guan, 2023) uses locality kernels for spatial adaptivity; RLCP (Hore and Barber, 2025) provides randomized guarantees; Mondrian CP (Vovk et al., 2005) achieves group-conditional coverage via partitioning. Optimization-based approaches (Gibbs et al., 2023) pursue group- or feature-conditional coverage; boosted CP (Xie et al., 2024) iteratively transforms scores to improve conditional coverage; self-calibrating CP (van der Laan and Alaa, 2024) targets prediction-conditional guarantees; and Plassier et al. (2025) provide non-asymptotic conditional coverage bounds. LWCP achieves approximate conditional coverage through closed-form geometric reweighting, limited to leverage-dependent heteroscedasticity (Theorem 3.12 quantifies when this suffices via η_{lev}). Bayesian-conformal hybrids (Cabezas et al., 2025) and CLAPS (Hobbhahn et al., 2025) use epistemic uncertainty estimates; Rossellini et al. (2024) decompose uncertainty into epistemic and aleatoric components for CQR—a decomposition that parallels LWCP+’s use of leverage and variance estimation. CLAPS’s Gram matrix $\Phi^\top \Phi$ is precisely the object from which our feature-space leverage is computed (Section A.8). CIR/CIR+ (Sesia and Romano, 2026) target distributional skewness—a different source of inefficiency than leverage-dependent scale. All these methods require auxiliary model training, kernel design, or posterior computation; LWCP requires none.

Leverage scores. Introduced in regression diagnostics (Chatterjee and Hadi, 1986, Hoaglin and Welsch, 1978),

leverage scores have found broad use in randomized numerical linear algebra (Drineas et al., 2006, 2012, Mahoney, 2011) and ridge regression (Alaoui and Mahoney, 2015). In GLMs, the *working leverage* governs prediction variance analogously (McCullagh and Nelder, 1989); we extend LWCP to this setting in Section D.3. For differentiable models, the *gradient leverage* captures prediction variance via the NTK linearization (Section D.4).

The closest prior use of leverage in conformal inference is Vovk’s RRCM (Burnaev and Vovk, 2014, Vovk et al., 2005), which uses LOO scores $|e_i|/(1-h_i)$ to correct training-side variance attenuation (Theorem 3.20, Part 1). LWCP instead corrects the test-side amplification by $(1+h)$ (Theorem 3.20, Part 2)—a distinction we formalize in Section A.8. Studentized scores (Lei et al., 2018) replace our closed-form $w(h)$ with a learned $\hat{\sigma}(x)$; local prediction bands (Lei and Wasserman, 2014) localize via kernel smoothing, while LWCP localizes through the one-dimensional projection $h(x)$, avoiding bandwidth selection. Under collinearity, ridge leverage provides principled stabilization (Section D.6). To our knowledge, leverage scores have not previously been used as conformal score weights.

2 LEVERAGE-WEIGHTED CONFORMAL PREDICTION

Setup. Data $\{(X_i, Y_i)\}_{i=1}^n$ with $X_i \in \mathbb{R}^p$, $Y_i \in \mathbb{R}$ are split into training \mathcal{D}_1 (n_1 points) and calibration \mathcal{D}_2 (n_2 points). Features are column-standardized using *training-set* statistics, applied identically to \mathcal{D}_2 and test points; intercepts are absorbed by centering. After standardization, the leverage score $h(x) = x^\top (\mathbf{X}_1^\top \mathbf{X}_1)^{-1} x$ equals the squared sample Mahalanobis distance from the training centroid, scaled by $1/n_1$. Preprocessing affects $h(x)$ values but not coverage (Theorem 3.1); we recommend column-standardization as default (Section E.5). The predictor \hat{f} is trained on \mathcal{D}_1 . Via the thin SVD $\mathbf{X}_1 = \mathbf{U}_1 \boldsymbol{\Sigma}_1 \mathbf{V}_1^\top$, leverage is computed as $h(x) = \|\boldsymbol{\Sigma}_1^{-1} \mathbf{V}_1^\top x\|_2^2$.

Definition 2.1 (Leverage-weighted nonconformity score). For a measurable function $w : [0, \infty) \rightarrow \mathbb{R}_+$, the leverage-weighted score is $V_w(x, y) = |y - \hat{f}(x)| \cdot w(h(x))$.

Definition 2.2 (LWCP prediction interval). The LWCP interval at level $1 - \alpha$ is

$$\hat{\mathcal{C}}_n^w(x) = \left[\hat{f}(x) - \frac{\hat{q}_w}{w(h(x))}, \hat{f}(x) + \frac{\hat{q}_w}{w(h(x))} \right], \quad (1)$$

where \hat{q}_w is the $\lceil (1 - \alpha)(n_2 + 1) \rceil$ -th smallest value among $\{V_w(X_i, Y_i)\}_{i \in \mathcal{D}_2}$.

The width at x is $2\hat{q}_w/w(h(x))$ (cf. Theorems 2.1 and 2.2). Choosing w decreasing in h gives wider intervals for high-leverage points (where prediction is harder) and narrower ones for low-leverage points.

Algorithm 1 Leverage-Weighted Conformal Prediction

Require: Data $\{(X_i, Y_i)\}_{i=1}^n$, test point x_{new} , level α , weight function w

- 1: Split data into \mathcal{D}_1 (n_1 pts) and \mathcal{D}_2 (n_2 pts)
- 2: Standardize features using \mathcal{D}_1 statistics (apply to \mathcal{D}_2 and x_{new})
- 3: Train predictor \hat{f} on \mathcal{D}_1 ; compute SVD $\mathbf{X}_1 = \mathbf{U}_1 \boldsymbol{\Sigma}_1 \mathbf{V}_1^\top$
- 4: **for** each $i \in \mathcal{D}_2$ **do**
- 5: $h_i \leftarrow \|\boldsymbol{\Sigma}_1^{-1} \mathbf{V}_1^\top \mathbf{X}_i\|_2^2$; $R_i \leftarrow |Y_i - \hat{f}(X_i)| \cdot w(h_i)$
- 6: **end for**
- 7: $\hat{q}_w \leftarrow \lceil (1 - \alpha)(n_2 + 1) \rceil$ -th smallest of $\{R_i\}_{i \in \mathcal{D}_2}$
- 8: $h_{\text{new}} \leftarrow \|\boldsymbol{\Sigma}_1^{-1} \mathbf{V}_1^\top x_{\text{new}}\|_2^2$
- 9: **return** $\hat{f}(x_{\text{new}}) \pm \hat{q}_w / w(h_{\text{new}})$

Canonical weighting functions. (1) **Constant** ($w(h) = 1$): recovers vanilla CP. (2) **Inverse-root leverage** ($w(h) = (1 + h)^{-1/2}$): matches the prediction variance structure $\sigma^2(1 + h)$ of OLS with homoscedastic errors. (3) **Power-law** ($w(h) = h^{-\gamma}$, $\gamma > 0$): tunable aggressiveness.

Computational cost. The full procedure (Algorithm 1) requires an SVD of \mathbf{X}_1 costing $O(n_1 p^2)$, or $O(n_1 p \log p)$ with randomized SVD. Leverage computation for n_2 calibration points costs $O(n_2 p)$. Total: $O(n_1 p^2 + n_2 p)$, with no hyperparameters beyond the choice of w .

LWCP+: Combining leverage with residual scale estimation. When heteroscedasticity has both leverage-dependent and feature-dependent components, we extend LWCP to **LWCP+** with composite scores:

$$s_i^+ = \frac{|Y_i - \hat{f}(X_i)|}{\hat{\sigma}(X_i) \cdot w(h(X_i))}, \quad (2)$$

where $\hat{\sigma} : \mathbb{R}^p \rightarrow \mathbb{R}_+$ is a lightweight scale estimator trained on \mathcal{D}_1 (e.g., a 10-tree random forest on training absolute residuals $\{(X_i, |Y_i - \hat{f}(X_i)|)\}_{i \in \mathcal{D}_1}$). The prediction interval at x has half-width $\hat{q}_{w,\sigma} \cdot \hat{\sigma}(x) / w(h(x))$, adapting to both input-space geometry (via h) and conditional noise scale (via $\hat{\sigma}$). LWCP+ recovers vanilla CP ($\hat{\sigma} \equiv 1, w \equiv 1$), LWCP ($\hat{\sigma} \equiv 1$), and studentized CP ($w \equiv 1$) as special cases. Since $\hat{\sigma}$ is \mathcal{D}_1 -measurable, marginal coverage is preserved exactly (Theorem 3.18).

3 THEORETICAL RESULTS

3.1 FINITE-SAMPLE MARGINAL COVERAGE

Theorem 3.1 (Marginal coverage). *Let (X_i, Y_i) , $i = 1, \dots, n + 1$, be exchangeable. For any predictor \hat{f} trained on \mathcal{D}_1 and any measurable $w : [0, \infty) \rightarrow \mathbb{R}_+$, the LWCP interval (1) satisfies $\mathbb{P}(Y_{n+1} \in \hat{\mathcal{C}}_n^w(X_{n+1}) \mid \mathcal{D}_1) \geq 1 - \alpha$.*

If scores are a.s. distinct, $\mathbb{P}(Y_{n+1} \in \hat{\mathcal{C}}_n^w(X_{n+1}) \mid \mathcal{D}_1) \leq 1 - \alpha + 1/(n_2 + 1)$.

Proof. Conditional on \mathcal{D}_1 (which determines \hat{f} and $h(\cdot)$), the scores $R_i = |Y_i - \hat{f}(X_i)| \cdot w(h(X_i))$ for $i \in \mathcal{D}_2 \cup \{n + 1\}$ are functions of exchangeable (X_i, Y_i) , hence exchangeable. By rank uniformity (Vovk et al., 2005, Lemma 8.1), the rank of R_{n+1} is uniform over $\{1, \dots, n_2 + 1\}$, giving $\mathbb{P}(R_{n+1} \leq \hat{q}_w \mid \mathcal{D}_1) \geq \lceil (1 - \alpha)(n_2 + 1) \rceil / (n_2 + 1) \geq 1 - \alpha$. When scores are a.s. distinct, $\mathbb{P} \leq 1 - \alpha + 1/(n_2 + 1)$. The proof makes *no assumptions* on P , \hat{f} , or w . \square \square

3.2 EFFICIENCY UNDER HETEROSCEDASTICITY

Assumption 3.2 (Linear model with leverage-dependent scale family). $Y_i = X_i^\top \beta^* + \varepsilon_i$ where $\varepsilon_i = \sigma \sqrt{g(h(X_i))} \cdot \eta_i$, $\eta_i \stackrel{iid}{\sim} F_\eta$, $\mathbb{E}[\eta_i] = 0$, $\text{Var}(\eta_i) = 1$, and $\{\eta_i\}$ are independent of $\{X_i\}$. The function $g : [0, \infty) \rightarrow \mathbb{R}_+$ is continuous, strictly increasing, with $g(0) > 0$.

This is stronger than specifying only the conditional variance: the *full conditional distribution* of $\varepsilon_i / \sqrt{g(h_i)}$ must be the same for all i , ensuring conditional quantiles of $|\varepsilon_i|$ scale with $\sqrt{g(h_i)}$.¹ We relax the scale-family assumption in Section D.1, providing explicit bounds under approximate scale families. The fixed- p assumption is relaxed in Theorem 3.16 (details in Section D.2), where we derive coverage guarantees in the proportional regime $p/n_1 \rightarrow \gamma \in (0, 1)$ using Marchenko–Pastur theory.

Assumption 3.3 (Regularity). As $n \rightarrow \infty$ with $n_1, n_2 \rightarrow \infty$ and p fixed: (a) $\|\hat{\beta} - \beta^*\| = O_p(1/\sqrt{n_1})$; (b) the empirical leverage distribution converges weakly to F_h ; (c) F_η is continuous.

The *variance-stabilized* weight is $w^*(h) = 1/\sqrt{g(h)}$. The intuition: under the scale family, $|\varepsilon_i| / \sqrt{g(h_i)} = \sigma |\eta_i|$, so dividing by $\sqrt{g(h_i)}$ yields scores that are not merely variance-stabilized but *identically distributed*. This scale-family structure is empirically well-motivated: in linear regression, the conditional distribution of $Y_i - X_i^\top \beta^*$ given X_i inherits its shape from F_η , with only the scale depending on leverage via $\sqrt{g(h_i)}$.

Theorem 3.4 (Efficiency of variance-stabilized LWCP). *Under Theorems 3.2 and 3.3:*

1. **(Conditional coverage.)** For F_h -a.e. h : $\mathbb{P}(Y_{n+1} \in \hat{\mathcal{C}}_n^{w^*}(X_{n+1}) \mid h(X_{n+1}) = h) \rightarrow 1 - \alpha$.

¹When heteroscedasticity does not factor through leverage alone, Theorem 3.12 quantifies the degradation: LWCP's gap reduction is $\sqrt{1 - \eta_{\text{lev}}}$, where η_{lev} measures the fraction of variance explained by leverage. LWCP+ (Section 3.7) addresses both leverage-dependent and feature-dependent components.

2. (**Width parity.**) $\mathbb{E}[|\hat{\mathcal{C}}_n^{w^*}(X_{n+1})|]/\mathbb{E}[|\hat{\mathcal{C}}_n^1(X_{n+1})|] \rightarrow 1$.
LWCP achieves conditional coverage at essentially no marginal width cost.

Proof sketch. **Part 1.** Under Theorem 3.3(a), $Y_i - \hat{f}(X_i) = \varepsilon_i + o_p(1)$ uniformly. The variance-stabilized scores $R_i^{w^*} = |\varepsilon_i + o_p(1)|/\sqrt{g(h_i)}$ are asymptotically iid under the scale-family Theorem 3.2, since $|\varepsilon_i|/\sqrt{g(h_i)} = \sigma|\eta_i|$. Thus $\hat{q}_{w^*} \rightarrow \sigma F_{|\eta|}^{-1}(1-\alpha)$, giving conditional coverage $\rightarrow 1-\alpha$ for all h . **Part 2.** Vanilla CP's quantile converges to $q_{\text{mix}} := Q_{1-\alpha}(\sigma\sqrt{g(H)}|\eta|)$; as $p/n \rightarrow 0$, leverages concentrate, the scale mixture degenerates, and the width ratio $\rightarrow 1$. Full proof in Section A.1. \square

Theorem 3.5 (Non-asymptotic width parity). *Under Theorems 3.2 and 3.3, let $\rho^2 = \text{CV}^2(\sqrt{g(H)})$. Then:*

$$\frac{\mathbb{E}_H[|\hat{\mathcal{C}}^{w^*}(X)|]}{\mathbb{E}_H[|\hat{\mathcal{C}}^1(X)|]} = 1 + C_\alpha \rho^2 + O(\rho^3) + O(1/\sqrt{n_2}),$$

where $C_\alpha = \frac{1}{2}(1 + q_\alpha f'_{|\eta|}(q_\alpha)/f_{|\eta|}(q_\alpha))$ with $q_\alpha = F_{|\eta|}^{-1}(1-\alpha)$. For Gaussian η : $C_\alpha = (1 - q_\alpha^2)/2 < 0$ whenever $\alpha < 0.32$, so LWCP is actually narrower than vanilla CP. For $g \equiv 1$: $\rho = 0$ and the ratio is exactly 1.

Proof sketch. Write $G = \sqrt{g(H)}$, $\mu_G = \mathbb{E}[G]$, and $G = \mu_G(1+\delta)$ with $\text{Var}(\delta) = \rho^2$. Taylor-expanding the scale-mixture quantile $Q_{1-\alpha}((1+\delta)|\eta|)$ around $\delta = 0$ gives C_α from the log-concavity correction $q_\alpha f'_{|\eta|}(q_\alpha)/f_{|\eta|}(q_\alpha)$. For Gaussian η , $f'_{|\eta|}(t) = -tf_{|\eta|}(t)$, yielding $C_\alpha = (1 - q_\alpha^2)/2$. Finite-sample correction is $O(1/\sqrt{n_2})$ via DKW. Full proof in Section A.3. \square

At $p/n_1 = 0.1$ with $g(h) = 1 + h$: $\rho^2 \approx 1.7 \times 10^{-4}$, consistent with observed ratios of 0.999–1.000 (Table 1).

Proposition 3.6 (Conditional coverage gap). *Under Theorems 3.2 and 3.3 with $w = w^*$: $\sup_h |\mathbb{P}(Y_{n+1} \in \hat{\mathcal{C}}_n^{w^*}(X_{n+1}) \mid h(X_{n+1}) = h) - (1 - \alpha)| = O(1/\sqrt{n_2}) + O(\sqrt{p/n_1})$.*

Proof sketch. The $O(1/\sqrt{n_2})$ term is the standard quantile estimation error (DKW inequality). The $O(\sqrt{p/n_1})$ term bounds $\|\hat{\beta} - \beta^*\| = O_p(\sqrt{p/n_1})$ from Theorem 3.3(a): the residuals $Y_i - \hat{f}(X_i) = \varepsilon_i + X_i^\top(\beta^* - \hat{\beta})$ differ from ε_i by this estimation error, which propagates through the score transformation. Proof in Section A.1. \square

Remark 3.7 (Relation to impossibility results). Distribution-free conditional coverage $\mathbb{P}(Y \in \hat{\mathcal{C}}(X) \mid X = x) \geq 1 - \alpha$ for all x is impossible in general (Barber et al., 2021b, Vovk, 2012). LWCP circumvents this by targeting a weaker but practically useful guarantee: coverage conditional on the *one-dimensional* projection $h(X)$, which suffices when heteroscedasticity factors through leverage (Theorem 3.2).

The scale family turns $h(X)$ into a sufficient statistic for the conditional distribution of $|Y - \hat{f}(X)|$, making conditional calibration feasible. This is analogous to Mondrian CP (Vovk et al., 2005), which achieves exact group-conditional coverage via finite partitions; LWCP achieves approximate h -conditional coverage via continuous reweighting.

The key insight is that w^* renders scores approximately iid, so the conformal quantile tracks the conditional quantile $Q_{1-\alpha}(\sigma|\eta|)$ uniformly in h . For vanilla CP, the scale mixture creates a persistent gap that does not vanish with sample size:

Theorem 3.8 (Persistent $\Theta(1)$ gap for vanilla CP). *Under Theorem 3.2 with g non-constant and Theorem 3.3, for any h_1, h_2 with $g(h_1) < g(h_2)$, the asymptotic conditional coverage difference $\Delta(h_1, h_2) > 0$ does not vanish with sample size. Quantitatively:*

$$\Delta(h_1, h_2) \geq f_{|\eta|}(q_\alpha) \cdot q_\alpha \cdot \frac{\sqrt{g(h_2)} - \sqrt{g(h_1)}}{\sqrt{g(h_2)}} \cdot (1 + o(1)).$$

For $g(h) = 1 + h$, Gaussian errors, $\alpha = 0.1$: $\Delta(h_{\min}, h_{\max}) = \Theta(h_{\max} - h_{\min})$.

Proof sketch. As $n \rightarrow \infty$, vanilla CP's quantile $\hat{q}_1 \rightarrow q_{\text{mix}} := Q_{1-\alpha}(\sigma\sqrt{g(H)}|\eta|)$. Conditional on leverage h , asymptotic coverage is $F_{|\eta|}(q_{\text{mix}}/(\sigma\sqrt{g(h)}))$. Since $F_{|\eta|}$ is strictly increasing and $g(h_1) \neq g(h_2)$, the coverage difference is positive and *independent of n* . The quantitative bound follows from the mean value theorem. Proof in Section A.4. \square

3.3 CLASSICAL RECOVERY

Theorem 3.9 (Gaussian recovery). *Under $Y_i = X_i^\top \beta^* + \varepsilon_i$ with $\varepsilon_i \stackrel{iid}{\sim} \mathcal{N}(0, \sigma^2)$ and $\hat{f} = \text{OLS}$, setting $w(h) = (1 + h)^{-1/2}$: as $n_1, n_2 \rightarrow \infty$ with p fixed, the LWCP interval width at x converges to $2\sigma z_{1-\alpha/2}\sqrt{1 + h(x)}$, recovering the form of the classical prediction interval (with z - vs. t -quantile and sample-splitting as finite-sample differences).*

Proof sketch. Under Gaussianity, the variance-stabilized scores $R_i^w = |Y_i - \hat{f}(X_i)|/\sqrt{1 + h_i}$ are distributed as $\sigma|Z_i|$ (iid half-normal), so $\hat{q}_w \rightarrow \sigma z_{1-\alpha/2}$, recovering the classical half-width $\sigma z_{1-\alpha/2}\sqrt{1 + h(x)}$. See Section A.1 for the complete argument. \square

3.4 APPROXIMATE LEVERAGE SCORES

Theorem 3.10 (Coverage under approximate leverage). *Let \tilde{h}_i be ϵ -approximate leverage scores $((1 - \epsilon)h_i \leq \tilde{h}_i \leq (1 + \epsilon)h_i)$. Then: (1) Marginal coverage is preserved exactly; (2) Width perturbation is bounded by $O(L\epsilon\|h\|_\infty/w_{\min})$ for L -Lipschitz w bounded below by w_{\min} .*

Such approximations are computable in $O(n_1 p \log p)$ time via randomized projections (Clarkson and Woodruff, 2013, Drineas et al., 2012, Woodruff, 2014); see Sections C.5 and C.12 for experiments.

Proof sketch. Part (1): \tilde{h} is computed from \mathcal{D}_1 alone, so $\tilde{w}(x) = w(\tilde{h}(x))$ is \mathcal{D}_1 -measurable. The exchangeability of $\{(X_i, Y_i)\}_{i \in \mathcal{D}_2 \cup \{n+1\}}$ conditional on \mathcal{D}_1 is unaffected, and Theorem 3.1 applies verbatim. Part (2): By Lipschitz continuity, $|w(\tilde{h}) - w(h)| \leq L|\tilde{h} - h| \leq L\epsilon h$; the width perturbation follows from bounding $w(h)/w(\tilde{h})$. Full proof in Section A.1. \square

3.5 OPTIMAL WEIGHT

Proposition 3.11 (Optimality of w^*). *Under Theorem 3.2, among all w achieving asymptotic conditional coverage for F_h -a.e. h , the variance-stabilized weight $w^*(h) = 1/\sqrt{g(h)}$ achieves minimum expected width.*

Proof in Section A.1: matching the LWCP half-width $\hat{q}_w/w(h)$ to the conditional quantile $\sigma\sqrt{g(h)}Q_{1-\alpha}(|\eta|)$ for all h forces $w(h) \propto 1/\sqrt{g(h)} = w^*(h)$.

3.6 ROBUSTNESS AND EXTENSIONS

The preceding theory assumes the scale-family model (Theorem 3.2). We now characterize LWCP under misspecification and extend to high-dimensional settings.

Theorem 3.12 (LWCP under general heteroscedasticity). *Let $\text{Var}(\varepsilon|X=x) = \sigma^2(x)$ be arbitrary (not necessarily leverage-dependent). Define $\sigma_h^2(h) := \mathbb{E}[\sigma^2(X) | h(X) = h]$ and $\eta_{\text{lev}} := \text{Var}(\sigma_h^2(H))/\text{Var}(\sigma^2(X)) \in [0, 1]$, measuring the fraction of variance heterogeneity explained by leverage. Then:*

1. **Marginal validity is preserved** regardless of misspecification.
2. **Gap comparison:** $\text{gap}_{\text{LWCP}}/\text{gap}_{\text{Vanilla}} \leq \sqrt{1 - \eta_{\text{lev}}} + O(1/\sqrt{n})$.

When $\eta_{\text{lev}} \approx 1$ (heteroscedasticity is leverage-driven), LWCP nearly eliminates the gap. When $\eta_{\text{lev}} \approx 0$ (heteroscedasticity is orthogonal to leverage), LWCP reduces to vanilla CP. In both cases, it never hurts marginal validity; under approximate scale families, explicit bounds are in Theorem D.2. Full gap decomposition in Section A.5.

Proof sketch. Part (i) is Theorem 3.1. For (ii), decompose $\sigma^2(x) = \sigma_h^2(h(x)) \cdot \psi^2(x)$ where $\mathbb{E}[\psi^2|h] = 1$. Under LWCP with $w(h) = 1/\sigma_h(h)$, the residual score heterogeneity is $\text{CV}(\psi|h)$ —the component orthogonal to leverage. By the law of total variance, $\text{Var}(\sigma^2(X)) = \text{Var}(\sigma_h^2(H)) +$

$\mathbb{E}[\text{Var}(\sigma^2(X)|H)]$, giving the stated ratio via η_{lev} . Quantile sensitivity (Theorem A.1) converts CV to gap. Proof in Section A.5. \square

Theorem 3.13 (Ridge-LWCP). *When $p \geq n_1$ or \mathbf{X}_1 is ill-conditioned, ridge leverage $h^\lambda(x) = x^\top(\mathbf{X}_1^\top \mathbf{X}_1 + \lambda \mathbf{I})^{-1}x$ with $\lambda > 0$ satisfies: (1) exact marginal coverage for any w and λ ; (2) well-posedness: $h^\lambda(x) \in [0, \|x\|^2/\lambda]$ is always finite; (3) under ridge regression, $\text{Var}(Y_{\text{new}} - \hat{f}_\lambda(x) | x) = \sigma^2(1 + h^\lambda(x)) + \lambda^2\|b_\lambda(x)\|^2$, where b_λ is the bias. Proof in Section B.*

The following proposition completes the robustness picture by characterizing the worst case for LWCP.

Proposition 3.14 (Adversarial worst case). *For “anti-aligned” heteroscedasticity $g_{\text{adv}}(h) = c/(1+h)$:*

1. *Marginal coverage is preserved exactly.*
2. *LWCP has worse conditional coverage than vanilla CP since total prediction variance is approximately constant.*
3. *General degradation bound:* $\text{gap}_{\text{LWCP}}^w - \text{gap}_{\text{LWCP}}^{w^*} \leq C_\alpha \cdot \text{CV}^2(\sqrt{(1+H)/g(H)})$. For g_{adv} , this is $O(p/n_1^2)$, making the degradation negligible for moderate p/n_1 .

Proof sketch. Part (i) is Theorem 3.1. Under g_{adv} , the optimal weight is $w^*(h) = \sqrt{(1+h)/c}$, which increases with h —opposite to LWCP’s $(1+h)^{-1/2}$. The degradation is $\text{CV}^2(w^*/w) = \text{CV}^2(1+H) = O(p/n_1^2)$ by concentration of Marchenko–Pastur leverage moments. Proof in Section A.6. \square

This adversarial scenario is highly unnatural—noise must decrease for extreme points—and the $\hat{\eta}$ diagnostic (Theorem 3.22) detects it. Our experiment confirms LWCP’s gap (2.0pp) \approx vanilla’s (2.1pp) even here (Table 1). More fundamentally, the default weight has bounded downside:

Proposition 3.15 (Safe default). *For any predictor \hat{f} , any distribution P , and $w(h) = (1+h)^{-1/2}$:*

1. *Marginal coverage $\geq 1 - \alpha$ holds exactly (Theorem 3.1).*
2. *Expected width:* $\mathbb{E}[|\hat{\mathcal{C}}^w|]/\mathbb{E}[|\hat{\mathcal{C}}^1|] = 1 + O(\text{CV}^2(H))$, i.e., within $O(1/n_1)$ of vanilla CP.
3. *Worst-case gap increase:* $\text{gap}^w - \text{gap}^1 \leq C_\alpha \cdot \text{CV}^2(H) = O(\gamma(1-\gamma)/n_1)$. At $\gamma=0.1$, $n_1=300$: <0.01 pp.

The downside is $O(1/n_1)$; the upside is $\Theta(1)$ when heteroscedasticity aligns with leverage.

Proof in Section D.5. The preceding theory assumes p fixed. Under proportional asymptotics ($p/n_1 \rightarrow \gamma$), LWCP’s advantage grows:

Proposition 3.16 (High-dimensional gap). *Under Theorem 3.2 with $g(h) = 1+h$ and $p/n_1 \rightarrow \gamma \in (0, 1)$:*

1. *Vanilla CP*: $\Delta_{\text{Vanilla}} = \Theta(\sqrt{\gamma(1-\gamma)/n_1})$.
2. *LWCP*: $\Delta_{\text{LWCP}} = O(1/\sqrt{n_2}) + O(\gamma/\sqrt{n_1})$.
3. *Ratio*: $\Delta_{\text{LWCP}}/\Delta_{\text{Vanilla}} \leq C/\sqrt{1+\gamma}$ for a universal constant $C < 1$, so LWCP strictly reduces the gap at all aspect ratios $\gamma \in (0, 1)$.

At $\gamma=0.9$, $n_1=300$: gap reduces from 12.4pp to 3.3pp ($3.8\times$; Table 18).

Proof via Marchenko–Pastur concentration in Section D.2; width parity is preserved (Theorem D.7). Fairness analysis (Theorem D.18) in Section D.7.

Remark 3.17 (Cross-conformal extension). LWCP extends to cross-conformal prediction (Vovk, 2015): for each fold k , compute the SVD of \mathbf{X}_{-k} and weight the residuals by $w(h_k(\cdot))$. Finite-sample validity is preserved by exchangeability, at cost $O(Kn_1p^2)$. See Section A.8.

3.7 LWCP+ THEORY

The efficiency results above require Theorem 3.2 (scale family). We now develop theory for LWCP+ that applies under weaker conditions.

Theorem 3.18 (LWCP+ marginal coverage). *Let (X_i, Y_i) , $i = 1, \dots, n+1$, be exchangeable. For any predictor \hat{f} and scale estimator $\hat{\sigma}$ both trained on \mathcal{D}_1 , and any measurable $w : [0, \infty) \rightarrow \mathbb{R}_+$, the LWCP+ interval with scores (2) satisfies $\mathbb{P}(Y_{n+1} \in \hat{\mathcal{C}}_n^{w, \hat{\sigma}}(X_{n+1}) \mid \mathcal{D}_1) \geq 1 - \alpha$.*

Proof sketch. Both $\hat{\sigma}(\cdot)$ and $w(h(\cdot))$ are \mathcal{D}_1 -measurable. Conditional on \mathcal{D}_1 , the composite scores s_i^+ for $i \in \mathcal{D}_2 \cup \{n+1\}$ are functions of exchangeable (X_i, Y_i) ; the argument of Theorem 3.1 applies verbatim. \square

Proposition 3.19 (Prediction variance decomposition). *Under a linear model $Y = X^\top \beta^* + \varepsilon$ with $\hat{f} = \text{OLS}$ on \mathcal{D}_1 , the prediction error at a new point x satisfies:*

$$\text{Var}(Y_{\text{new}} - \hat{f}(x) \mid x, \mathcal{D}_1) = \underbrace{\text{Var}(\varepsilon_{\text{new}} \mid x)}_{\text{noise}} + \underbrace{\sigma_{\text{OLS}}^2 \cdot h(x)}_{\text{estimation}}.$$

LWCP corrects the second term; studentized CP targets the first; LWCP+ addresses both.

Proof sketch. Write $Y_{\text{new}} - \hat{f}(x) = \varepsilon_{\text{new}} - x^\top(\hat{\beta} - \beta^*)$. Independence of ε_{new} and $\hat{\beta} - \beta^*$ gives variance additivity. Under homoscedastic errors, $\text{Cov}(\hat{\beta} \mid \mathbf{X}_1) = \sigma^2(\mathbf{X}_1^\top \mathbf{X}_1)^{-1}$, so $x^\top \text{Cov}(\hat{\beta})x = \sigma^2 h(x)$. Proof in Section A.1. \square

Proposition 3.20 (Training-test variance mismatch). *Under the homoscedastic linear model ($\varepsilon_i \stackrel{iid}{\sim} (0, \sigma^2)$, $\hat{f} = \text{OLS}$):*

1. **Training residuals:** $\text{Var}(Y_i - \hat{f}(X_i) \mid \mathbf{X}_1) = \sigma^2(1 - h_i)$ for $i \in \mathcal{D}_1$.

2. **Prediction errors:** $\text{Var}(Y_{\text{new}} - \hat{f}(x) \mid x, \mathbf{X}_1) = \sigma^2(1 + h(x))$ for new x .

The sign of the leverage contribution flips: training residuals are attenuated at high leverage (factor $1 - h$), while prediction errors are amplified (factor $1 + h$).

Proof sketch. Part 1: Write $e_i^{\text{train}} = ((I - \mathbf{H})\varepsilon_1)_i$, where $\mathbf{H} = \mathbf{X}_1(\mathbf{X}_1^\top \mathbf{X}_1)^{-1}\mathbf{X}_1^\top$ is idempotent. Then $\text{Var}(e_i) = \sigma^2(I - \mathbf{H})_{ii} = \sigma^2(1 - h_i)$. Part 2: For $i \in \mathcal{D}_2$, $\varepsilon_{\text{new}} \perp\!\!\!\perp \varepsilon_1$, so variances add: $\sigma^2 + \sigma^2 h(x) = \sigma^2(1 + h(x))$. Proof in Section A.1. \square

Corollary 3.21 (LWCP+ corrects the mismatch). *A scale estimator $\hat{\sigma}$ trained on $\{(X_i, |\varepsilon_i^{\text{train}}|)\}_{i \in \mathcal{D}_1}$ approximates $\sigma\sqrt{1 - h(\cdot)}$, not $\sigma\sqrt{1 + h(\cdot)}$. Studentized CP has h -dependent factor $\phi_S(h) = \sqrt{(1+h)/(1-h)}$; LWCP+ divides additionally by $\sqrt{1+h}$, giving factor $\phi_+(h) = 1/\sqrt{1-h}$. The CV² ratio is:*

$$\frac{\text{CV}^2(\phi_S(H))}{\text{CV}^2(\phi_+(H))} = \frac{4}{(1 + \bar{h})^2} + O(\text{Var}(H)), \quad \bar{h} = p/n_1.$$

For $p/n_1 \rightarrow 0$ this approaches 4: LWCP+ reduces the h -dependent score variability by $4\times$ (in CV²), giving $\approx 2\times$ smaller conditional gap than studentized CP (Theorem A.4).

The factor of 4 has a clean explanation: Studentized CP's score is affected by leverage through *both* numerator ($\sqrt{1+h}$) and denominator ($\sqrt{1-h}$), giving log-sensitivity $d \ln \phi_S/dh = 1/(1-h^2)$. LWCP+'s $\sqrt{1+h}$ correction cancels the numerator, halving the log-sensitivity to $1/(2(1-h))$. Since CV² scales as the square of log-sensitivity, the ratio is $2^2 = 4$.

Remark 3.22 (Diagnostics and robustness). The coefficient of variation $\hat{\eta} = \text{std}(h)/\text{mean}(h)$ is a practical diagnostic: $\hat{\eta} > 1$ indicates LWCP improves conditional coverage; $\hat{\eta} < 0.5$ indicates vanilla CP suffices. Under misspecification (Theorem 3.12), LWCP corrects only the leverage-dependent component, reducing the gap by $\sqrt{1 - \eta_{\text{lev}}}$. Marginal validity is always preserved.

Remark 3.23 (Feature-space leverage for non-linear models). For predictors \hat{f} linear in learned features $\phi(x)$ (e.g., last-layer neural networks), the feature-space leverage $h^\phi(x) = \phi(x)^\top(\Phi^\top \Phi + \lambda \mathbf{I})^{-1}\phi(x)$ inherits the coverage guarantee (Theorem 3.1) since it is \mathcal{D}_1 -measurable (Theorem B.1); analogues for GLMs (Theorem D.9) and gradient leverage (Theorem D.11) are in Section D. In the NTK/lazy regime, the efficiency theory (Theorem 3.4) applies to the last-layer linearization (Section A.8 and Theorem B.2). When $p \geq n_1$, ridge leverage (Theorem 3.13) ensures well-posedness.

Table 1: Marginal Coverage (Mean \pm Std, 1,000 Reps), Width Ratio, and Conditional Gap (200 Reps).

DGP	Marginal Coverage		Width Ratio	Cond. Gap	
	Vanilla	LWCP		Van.	LWCP
Textbook	.900 \pm .019	.900 \pm .019	1.000	2.7pp	1.3pp
Heavy-tailed	.900 \pm .019	.900 \pm .019	0.999	2.3pp	1.2pp
Polynomial	.900 \pm .020	.900 \pm .020	0.999	2.2pp	1.1pp
Homoscedastic	.900 \pm .019	.900 \pm .019	1.000	4.5pp	0.1pp
Adversarial	.900 \pm .019	.900 \pm .019	1.000	2.1pp	2.0pp

4 EXPERIMENTS

We evaluate LWCP with OLS as \hat{f} and $w(h) = (1+h)^{-1/2}$. Default parameters: $n_1 = 300$, $n_2 = 500$, $p = 30$, $\sigma = 1$, $\alpha = 0.1$ (90% nominal coverage), giving $p/n_1 = 0.1$.

Data-generating processes. Five DGPs with $X \sim \mathcal{N}(0, \Sigma)$, $\Sigma = \text{diag}(1, 1/2, \dots, 1/p)$: (1) **Textbook**: $\varepsilon | X \sim \mathcal{N}(0, \sigma^2(1+h))$, matching the weight function; (2) **Heavy-tailed**: same variance structure but t_3 errors; (3) **Polynomial**: degree-8 polynomial features with $g(h) = 1 + h$; (4) **Homoscedastic**: $\varepsilon \sim \mathcal{N}(0, \sigma^2)$, the null case; (5) **Adversarial**: $\text{Var}(\varepsilon | X) \propto 1 + \|X\|^2/p$, misspecified for LWCP (Theorem 3.14).

4.1 COVERAGE RESULTS

Table 1 confirms marginal coverage is preserved across all DGPs, with width ratio 0.999–1.000 (distributions in Section C.8). The homoscedastic DGP exhibits the largest conditional gap reduction (4.5pp to 0.1pp), consistent with the theory: $(1+h)^{-1/2}$ exactly stabilizes the prediction variance $\sigma^2(1+h)$.

4.2 CONDITIONAL COVERAGE

Figure 1 visualizes the central finding. Under homoscedastic errors ($g \equiv 1$), OLS prediction variance is exactly $\sigma^2(1+h)$, and LWCP’s weight $(1+h)^{-1/2}$ perfectly stabilizes it, yielding nearly flat conditional coverage. Under heteroscedastic DGPs ($p/n_1 = 0.1$), LWCP approximately halves the conditional gap. See Section C.2 for sensitivity sweeps and Section C.3 for width-vs-leverage scatter plots.

4.3 ADAPTIVE WIDTHS

LWCP redistributes width—wider for high-leverage points, narrower for low-leverage—with negligible net change (Figure 5). We compare against CQR (Romano et al., 2019), studentized CP (Papadopoulos et al., 2008), and localized CP (Guan, 2023) in Table 2 and fig. 2; configurations and runtime details are in Section C.13.

Table 2: MSCE ($\times 10^3$; \downarrow) Across Methods and DGPs (20 Reps). All methods achieve $\approx .90$ coverage.

Method	MSCE			
	Text.	Poly.	Adv.	Time
Vanilla CP	2.21	2.41	2.26	0.001s
LWCP	2.18	2.37	2.15	0.001s
CQR	1.94	2.82	2.01	0.170s
Studentized	1.99	3.76	2.11	0.127s
Localized	2.16	2.55	2.18	0.023s

Table 3: Real-Data Summary (10 Reps). Gap = $|\text{cov}(\text{low-}h) - \text{cov}(\text{high-}h)|$. MSCE ($\times 10^3$; \downarrow). Full comparison in Section C.6.

Method	CPU ($\hat{\eta} = 2.96$)			Diabetes ($\hat{\eta} = 0.67$)		
	Cov	Gap	MSCE	Cov	Gap	MSCE
Vanilla CP	.899	.189	6.59	.899	.061	6.41
LWCP	.899	.188	6.49	.900	.056	6.02
LWCP+	.903	.075	1.61	.913	.067	8.32
Studentized	.905	.084	2.05	.898	.078	10.7

Theorem 3.9 is validated at $n=1000$: the LWCP/classical width ratio is 1.002 ± 0.046 (Section C.1), and the gap convergence rate of Theorem 3.6 is confirmed in Section C.4.

4.4 BEYOND SYNTHETIC DATA

We evaluate on four real-world datasets (10 reps). Table 3 summarizes the two most informative; the full comparison is in Section C.6. On CPU Activity ($\hat{\eta} = 2.96$), LWCP+ substantially reduces both the conditional gap and MSCE, outperforming Studentized CP at lower computational cost—confirming the mismatch theory (Theorem 3.21). On Diabetes ($\hat{\eta} = 0.67$), LWCP achieves the lowest MSCE. When $\hat{\eta}$ is small, LWCP reduces to vanilla CP, validating the diagnostic (Theorem 3.22).

4.5 NON-LINEAR PREDICTORS

We evaluate with Random Forest (RF; Lin and Jeon, 2006) using raw-X leverage and MLP (feature-space leverage h^{NN} ; Theorem 3.23) on a non-linear DGP ($Y = \sum_j \sin(X_j) + \varepsilon$, 10 reps). Coverage holds for any \hat{f} (Theorem 3.1); LWCP reduces conditional gaps across all predictor types, with feature-space leverage providing the largest improvement. Full results in Section C.9.

4.6 PRACTICAL RECOMMENDATIONS

The diagnostic $\hat{\eta} = \text{std}(h)/\text{mean}(h)$ guides method selection: $\hat{\eta} > 1$ indicates LWCP improves conditional coverage;

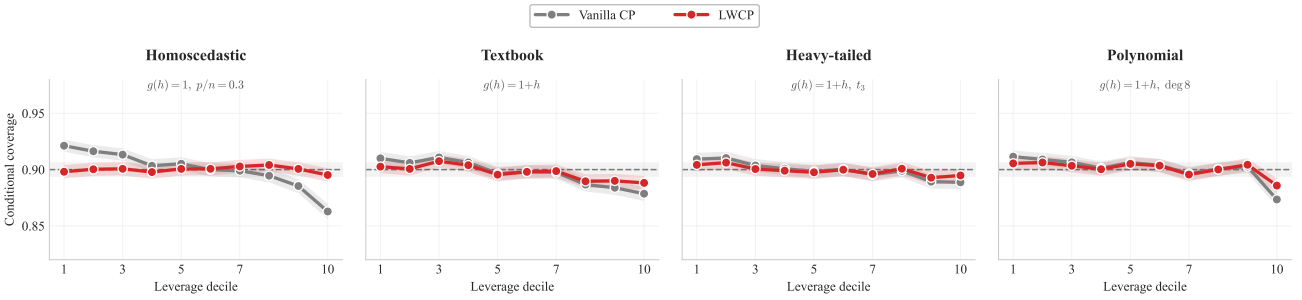


Figure 1: **Conditional coverage by leverage decile** (200 replications). Vanilla CP (gray) exhibits monotone undercoverage at high leverage. LWCP (red) achieves approximately flat conditional coverage across all DGPs, with the largest improvement under homoscedastic errors ($p/n_1 = 0.3$) where $(1+h)^{-1/2}$ exactly stabilizes the prediction variance.

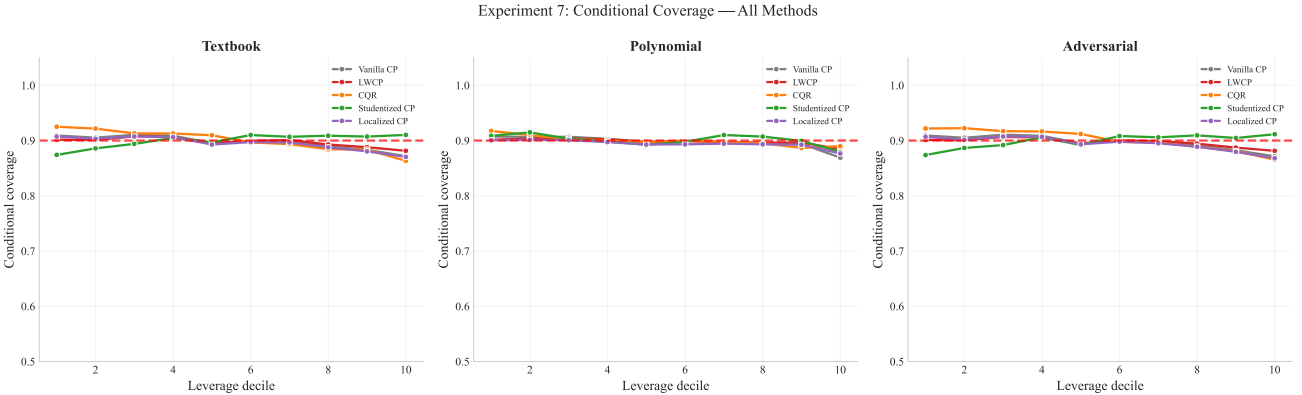


Figure 2: **Conditional coverage across methods**. LWCP (red) achieves the flattest coverage profile at the lowest computational cost. CQR (orange) attains comparable flatness but with substantially wider intervals. Studentized CP (green) achieves moderate improvement at significantly higher runtime.

$\hat{\eta} < 0.5$ indicates vanilla CP suffices. The default weight $w(h) = (1+h)^{-1/2}$ is provably safe (Theorem 3.15) and near-optimal across DGPs (Section E.3). Data-driven weight selection via a three-way split preserves coverage exactly, since the selected weight is \mathcal{D}_1 -measurable (Section C.11). Features should be standardized before computing leverage (Algorithm 1); points with $h(x)$ above the 99th calibration percentile should be flagged. Extended guidance on high-dimensional settings, covariate shift (Theorem B.4), collinearity (Theorem D.15), and extrapolation guardrails is in Section C.14. Additional experiments—ridge leverage at p/n_1 up to 10 (Section E.2), runtime benchmarking (Section E.1), LWCP+ vs. Studentized CP (Section E.4), and preprocessing ablation (Section E.5)—are in the supplement.

5 CONCLUSION

LWCP provides adaptive prediction intervals that are distribution-free, finite-sample valid for any weight function (Theorem 3.1), and achieve asymptotically optimal conditional coverage at negligible width cost (Theorems 3.4 and 3.5). The method adds no hyperparameters and scales

identically to vanilla CP. We established that vanilla CP suffers a persistent $\Theta(1)$ conditional coverage gap (Theorem 3.8), while LWCP eliminates this gap under the scale-family model. The default weight $(1+h)^{-1/2}$ is provably safe— $O(1/n_1)$ downside with $\Theta(1)$ upside (Theorem 3.15)—and LWCP’s advantage grows with $\gamma = p/n_1$ (Theorem 3.16). LWCP+ corrects the training-test variance mismatch limiting studentized CP (Theorem 3.21); under misspecification, the gap reduction is controlled by η_{lev} (Theorem 3.12).

References

- A. E. Alaoui and M. W. Mahoney. Fast randomized kernel ridge regression with statistical guarantees. In *Advances in Neural Information Processing Systems*, pages 775–783, 2015.
- S. I. Amoukou and N. J. B. Brunel. Adaptive conformal prediction by reweighting nonconformity score. *arXiv preprint arXiv:2303.12695*, 2023.
- R. F. Barber, E. J. Candès, A. Ramdas, and R. J. Tibshirani. Predictive inference with the jackknife+. *The Annals of Statistics*, 49(1):486–507, 2021a.

R. F. Barber, E. J. Candès, A. Ramdas, and R. J. Tibshirani. The limits of distribution-free conditional predictive inference. *Information and Inference*, 10(2):455–482, 2021b.

E. Burnaev and V. Vovk. Efficiency of conformalized ridge regression. In *Conference on Learning Theory (COLT)*, pages 605–622, 2014.

L. M. Cabezas, E. Creager, and G. Loaiza-Ganem. EPIC-SCORE: Epistemic uncertainty of conformal scores. *arXiv preprint arXiv:2501.13458*, 2025.

S. Chatterjee and A. S. Hadi. Influential observations, high leverage points, and outliers in linear regression. *Statistical Science*, 1(3):379–393, 1986.

K. L. Clarkson and D. P. Woodruff. Low rank approximation and regression in input sparsity time. In *Proceedings of the Forty-Fifth Annual ACM Symposium on Theory of Computing*, pages 81–90, 2013.

P. Drineas, M. W. Mahoney, and S. Muthukrishnan. Sampling algorithms for ℓ_2 regression and applications. In *Proceedings of the Seventeenth Annual ACM-SIAM Symposium on Discrete Algorithms*, pages 1127–1136, 2006.

P. Drineas, M. Magdon-Ismail, M. W. Mahoney, and D. P. Woodruff. Fast approximation of matrix coherence and statistical leverage. *Journal of Machine Learning Research*, 13:3475–3506, 2012.

I. Gibbs, J. J. Cherian, and E. J. Candès. Conformal prediction with conditional guarantees. *arXiv preprint arXiv:2305.12616*, 2023.

L. Guan. Localized conformal prediction: a generalized inference framework for conformal prediction. *Biometrika*, 110(1):33–50, 2023.

D. C. Hoaglin and R. E. Welsch. The hat matrix in regression and ANOVA. *The American Statistician*, 32(1):17–22, 1978.

M. Hobbhahn, A. Kristiadi, and P. Hennig. CLAPS: Posterior-aware conformal intervals via last-layer Laplace. *arXiv preprint arXiv:2512.01384*, 2025.

R. Hore and R. F. Barber. Conformal prediction with local weights: randomization enables robust guarantees. *Journal of the Royal Statistical Society Series B*, 87(2):549–578, 2025.

J. Lei and L. Wasserman. Distribution-free prediction bands for non-parametric regression. *Journal of the Royal Statistical Society: Series B*, 76(1):71–96, 2014.

J. Lei, M. G’Sell, A. Rinaldo, R. J. Tibshirani, and L. Wasserman. Distribution-free predictive inference for regression. *Journal of the American Statistical Association*, 113(523):1094–1111, 2018.

Y. Lin and Y. Jeon. Random forests and adaptive nearest neighbors. *Journal of the American Statistical Association*, 101(474):578–590, 2006.

M. W. Mahoney. Randomized algorithms for matrices and data. *Foundations and Trends in Machine Learning*, 3(2):123–224, 2011.

P. McCullagh and J. A. Nelder. *Generalized Linear Models*. Chapman & Hall/CRC, 2nd edition, 1989.

H. Papadopoulos, K. Proedrou, V. Vovk, and A. Gammerman. Inductive confidence machines for regression. In *European Conference on Machine Learning*, pages 345–356, 2002.

H. Papadopoulos, V. Vovk, and A. Gammerman. Normalized nonconformity measures for regression conformal prediction. In *Proceedings of the IASTED International Conference on Artificial Intelligence and Applications*, pages 64–69, 2008.

V. Plassier, B.-S. Makni, A. Rubashevskii, A. Novikov, and A. Kroshnin. Probabilistic conformal prediction with approximate conditional validity. In *International Conference on Learning Representations (ICLR)*, 2025.

A. Rahimi and B. Recht. Random features for large-scale kernel machines. In *Advances in Neural Information Processing Systems*, pages 1177–1184, 2007.

Y. Romano, E. Patterson, and E. Candès. Conformalized quantile regression. In *Advances in Neural Information Processing Systems*, pages 3543–3553, 2019.

R. Rossellini, R. F. Barber, and R. Willett. Integrating uncertainty awareness into conformalized quantile regression. In *International Conference on Artificial Intelligence and Statistics (AISTATS)*, volume 238 of *PMLR*, 2024.

M. Sesia and Y. Romano. Fast conformal prediction using conditional interquantile intervals. *arXiv preprint arXiv:2601.02769*, 2026.

G. Shafer and V. Vovk. A tutorial on conformal prediction. *Journal of Machine Learning Research*, 9:371–421, 2008.

G. R. Shorack and J. A. Wellner. *Empirical Processes with Applications to Statistics*. SIAM, 2009.

R. J. Tibshirani. Conformal prediction: A gentle introduction. *Foundations and Trends in Machine Learning*, 16(4):494–591, 2023.

R. J. Tibshirani, R. F. Barber, E. J. Candès, and A. Ramdas. Conformal prediction under covariate shift. In *Advances in Neural Information Processing Systems*, pages 2530–2540, 2019.

L. van der Laan and A. Alaa. Self-calibrating conformal prediction. In *Advances in Neural Information Processing Systems*, 2024.

A. W. van der Vaart. *Asymptotic Statistics*. Cambridge University Press, 2000.

V. Vovk. Conditional validity of inductive conformal predictors. In *Asian Conference on Machine Learning*, pages 475–490, 2012.

V. Vovk. Cross-conformal predictors. *Annals of Mathematics and Artificial Intelligence*, 74(1-2):9–28, 2015.

V. Vovk, A. Gammerman, and G. Shafer. *Algorithmic Learning in a Random World*. Springer, 2005.

V. Vovk, I. Petej, I. Nouretdinov, V. Manokhin, and A. Gammerman. Cross-conformal predictive distributions. In

Conformal and Probabilistic Prediction and Applications,
pages 37–51, 2018.

D. P. Woodruff. Sketching as a tool for numerical linear algebra. *Foundations and Trends in Theoretical Computer Science*, 10(1–2):1–157, 2014.

Y. Xie, R. F. Barber, and E. J. Candès. Boosted conformal prediction intervals. In *Advances in Neural Information Processing Systems*, 2024.

Leverage-Weighted Conformal Prediction (Supplementary Material)

Shreyas Fadnavis¹

¹shreyasfadnavis@gmail.com

The supplement is organized as follows. Section A contains all deferred proofs and extended theoretical results (coverage, efficiency, width parity, persistent gap, misspecification, adversarial analysis, and connections to related methods). Section B develops extensions to ridge regression, kernel methods, neural networks, and covariate shift. Section C presents additional experimental results including Gaussian recovery, heteroscedasticity sensitivity, scaling behavior, real-data benchmarks, and practical guidance. Section D provides deeper theoretical analysis on approximate scale families, high-dimensional asymptotics, GLMs, gradient leverage, leverage stability, and fairness. Section E contains supplementary runtime benchmarks, high-dimensional stress tests, weight comparisons, and preprocessing ablations.

A PROOFS AND EXTENDED THEORY

A.1 PROOFS OF MAIN-TEXT RESULTS

The following proofs are deferred from the main text for space. They are presented in theorem-number order. Supporting lemmas are in Section A.2; the quantitative mismatch analysis is in Section A.7.

Proof of Theorem 3.18. Both $\hat{o}(\cdot)$ and $w(h(\cdot))$ are functions of \mathcal{D}_1 alone. Conditional on \mathcal{D}_1 , the composite scores $s_i^+ = |Y_i - \hat{f}(X_i)|/(\hat{o}(X_i) \cdot w(h(X_i)))$ for $i \in \mathcal{D}_2 \cup \{n+1\}$ are functions of (X_i, Y_i) applied to exchangeable random variables. The argument of Theorem 3.1 applies verbatim. \square \square

Proof of Theorem 3.10. Part 1. Approximate leverage scores \tilde{h} are computed entirely from \mathcal{D}_1 , so $\tilde{w}(x) = w(\tilde{h}(x))$ is \mathcal{D}_1 -measurable. The exchangeability argument of Theorem 3.1 applies without modification, yielding exact coverage.

Part 2. The width at x changes from $2\hat{q}_w/w(h(x))$ to $2\hat{q}_{\tilde{w}}/w(\tilde{h}(x))$. By Lipschitz continuity, $|w(\tilde{h}) - w(h)| \leq L|\tilde{h} - h| \leq L\epsilon h$, giving $w(h)/w(\tilde{h}) = 1 + O(L\epsilon\|h\|_\infty/w_{\min})$. For the quantile perturbation, assuming the score density f_S satisfies $f_S(Q_{1-\alpha}(S)) \geq c > 0$ (a standard regularity condition), the quantile perturbation lemma (van der Vaart, 2000, Lemma 21.2) gives $|Q_{1-\alpha}(\tilde{S}) - Q_{1-\alpha}(S)| \leq \|F_S - F_{\tilde{S}}\|_\infty/c$. \square \square

Proof of Theorem 3.6. For LWCP with w^* , the variance-stabilized scores $R_i^{w^*} \approx \sigma|\eta_i|$ are approximately iid under Theorem 3.2. The conformal quantile \hat{q}_{w^*} estimates $Q_{1-\alpha}(\sigma|\eta|)$ with standard quantile estimation error $O(1/\sqrt{n_2})$, while the approximation $R_i^{w^*} \approx \sigma|\eta_i|$ incurs $O(\|\hat{\beta} - \beta^*\|) = O(\sqrt{p/n_1})$ error from Theorem 3.3(a). The conditional coverage at leverage h converges to $F_{|\eta|}(F_{|\eta|}^{-1}(1-\alpha)) = 1 - \alpha$ uniformly.

For vanilla CP, scores $R_i^1 = |\varepsilon_i + o_p(1)|$ have h -dependent distributions. The conformal quantile estimates $q_{\text{mix}} = Q_{1-\alpha}(\sigma\sqrt{g(H)}|\eta|)$, while the conditional $(1-\alpha)$ -quantile at leverage h is $\sigma\sqrt{g(h)}Q_{1-\alpha}(|\eta|)$. Since $\mathbb{E}_H[F_H(q_{\text{mix}})] = 1 - \alpha$ but F_h varies with h when g is non-constant, the gap between extreme leverages is (see Theorem 3.8):

$$\Delta(h_{\min}, h_{\max}) \geq f_{|\eta|}(q_\alpha) \cdot q_\alpha \cdot \frac{\sqrt{g(h_{\max})} - \sqrt{g(h_{\min})}}{\sqrt{g(h_{\max})}} = \Theta(h_{\max} - h_{\min}),$$

which does not vanish with n . \square \square

Proof of Theorem 3.9. For $i \in \mathcal{D}_2$, write $Y_i - \hat{f}(X_i) = \varepsilon_i - X_i^\top(\hat{\beta} - \beta^*)$. Since $\hat{\beta} - \beta^* = (\mathbf{X}_1^\top \mathbf{X}_1)^{-1} \mathbf{X}_1^\top \varepsilon_1 \sim \mathcal{N}(0, \sigma^2(\mathbf{X}_1^\top \mathbf{X}_1)^{-1})$ is independent of ε_i for $i \in \mathcal{D}_2$:

$$Y_i - \hat{f}(X_i) \mid X_i, \mathcal{D}_1 \sim \mathcal{N}(0, \sigma^2(1 + h_i)).$$

With $w(h) = (1 + h)^{-1/2}$, the scores $R_i^w = |Y_i - \hat{f}(X_i)|/\sqrt{1 + h_i} \sim \sigma|Z_i|$ where $Z_i \stackrel{iid}{\sim} \mathcal{N}(0, 1)$. The $(1 - \alpha)$ -quantile of $\sigma|Z_i|$ is $\sigma z_{1-\alpha/2}$, so $\hat{q}_w \rightarrow \sigma z_{1-\alpha/2}$. The LWCP half-width at x is $\sigma z_{1-\alpha/2} \sqrt{1 + h(x)}$, matching the classical prediction interval form. Finite-sample differences are: (i) $z_{1-\alpha/2}$ vs. $t_{n_1-p, 1-\alpha/2}$; (ii) sample splitting. Crucially, Theorem 3.1 guarantees finite-sample coverage *without* requiring the Gaussian assumption. \square \square

Proof of Theorem 3.19. Write $Y_{\text{new}} - \hat{f}(x) = \varepsilon_{\text{new}} - x^\top(\hat{\beta} - \beta^*)$. Since $\varepsilon_{\text{new}} \perp\!\!\!\perp (\hat{\beta} - \beta^*)$ conditional on x and \mathcal{D}_1 :

$$\text{Var}(Y_{\text{new}} - \hat{f}(x) \mid x, \mathcal{D}_1) = \text{Var}(\varepsilon_{\text{new}} \mid x) + x^\top \text{Cov}(\hat{\beta} \mid \mathbf{X}_1)x.$$

Under homoscedastic errors, $\text{Cov}(\hat{\beta} \mid \mathbf{X}_1) = \sigma^2(\mathbf{X}_1^\top \mathbf{X}_1)^{-1}$, so $x^\top \text{Cov}(\hat{\beta})x = \sigma^2 h(x)$. \square \square

Proof of Theorem 3.20. Part 1. Write $\hat{\beta} = (\mathbf{X}_1^\top \mathbf{X}_1)^{-1} \mathbf{X}_1^\top \mathbf{Y}_1 = \beta^* + (\mathbf{X}_1^\top \mathbf{X}_1)^{-1} \mathbf{X}_1^\top \varepsilon_1$. For $i \in \mathcal{D}_1$:

$$Y_i - \hat{f}(X_i) = ((I - \mathbf{H})\varepsilon_1)_i,$$

where $\mathbf{H} = \mathbf{X}_1(\mathbf{X}_1^\top \mathbf{X}_1)^{-1} \mathbf{X}_1^\top$. Since $\text{Var}(\varepsilon_1) = \sigma^2 I$ and $(I - \mathbf{H})$ is idempotent: $\text{Var}(e_i^{\text{train}}) = \sigma^2(1 - h_i)$.

Part 2. For $i \in \mathcal{D}_2$ (independent of \mathcal{D}_1), $\varepsilon_{\text{new}} \perp\!\!\!\perp \varepsilon_1$, so: $\text{Var}(Y_{\text{new}} - \hat{f}(x) \mid x, \mathbf{X}_1) = \sigma^2(1 + h(x))$. \square \square

Proof of Theorem 3.11. Under the scale-family Theorem 3.2, $|\varepsilon_i| \mid h_i \sim \sigma \sqrt{g(h_i)} \cdot |\eta_i|$. For any weight w to achieve asymptotic conditional coverage at level $1 - \alpha$ for F_h -a.e. h , the LWCP half-width $\hat{q}_w/w(h)$ must equal the conditional quantile $\sigma \sqrt{g(h)} \cdot Q_{1-\alpha}(|\eta_i|)$ asymptotically. Since the h -dependence is only through $1/w(h)$ vs. $\sqrt{g(h)}$, this forces $w(h) \propto 1/\sqrt{g(h)} = w^*(h)$. \square \square

Proof of Theorem 3.4. We prove the two parts in full.

Part 1 (Conditional coverage). Fix $h_0 \in \text{supp}(F_h)$. We show $\mathbb{P}(Y_{n+1} \in \hat{\mathcal{C}}_n^{w^*}(X_{n+1}) \mid h(X_{n+1}) = h_0) \rightarrow 1 - \alpha$.

Step 1: Score approximation. For $i \in \mathcal{D}_2$, write

$$Y_i - \hat{f}(X_i) = \varepsilon_i - X_i^\top(\hat{\beta} - \beta^*) = \sigma \sqrt{g(h_i)} \eta_i - X_i^\top(\hat{\beta} - \beta^*).$$

Under Theorem 3.3(a), $\|\hat{\beta} - \beta^*\| = O_p(1/\sqrt{n_1})$, so $|X_i^\top(\hat{\beta} - \beta^*)| = O_p(\|X_i\|/\sqrt{n_1})$. Since $\|X_i\|^2/p \rightarrow_p 1$ and p is fixed, $|X_i^\top(\hat{\beta} - \beta^*)| = O_p(1/\sqrt{n_1})$ uniformly over i . The variance-stabilized scores satisfy:

$$R_i^{w^*} = \frac{|Y_i - \hat{f}(X_i)|}{\sqrt{g(h_i)}} = \sigma |\eta_i| + O_p(1/\sqrt{n_1}) \quad \text{uniformly over } i \in \mathcal{D}_2.$$

Step 2: Quantile convergence. Since $R_i^{w^*} = \sigma |\eta_i| + o_p(1)$ and the η_i are iid with continuous distribution F_η (Theorem 3.3(c)), the empirical CDF of $\{R_i^{w^*}\}_{i \in \mathcal{D}_2}$ converges uniformly to $F_{\sigma|\eta|}$ by the Glivenko–Cantelli theorem (Shorack and Wellner, 2009, Chapter 14). The conformal quantile \hat{q}_{w^*} is the $\lceil (1 - \alpha)(n_2 + 1) \rceil / (n_2 + 1)$ -th quantile of this empirical distribution, so:

$$\hat{q}_{w^*} \rightarrow \sigma \cdot Q_{1-\alpha}(|\eta|) =: \sigma q_\alpha \quad \text{in probability.}$$

Step 3: Uniform conditional coverage. Conditional on $h(X_{n+1}) = h_0$, coverage is:

$$\begin{aligned} \mathbb{P}(Y_{n+1} \in \hat{\mathcal{C}}_n^{w^*} \mid h = h_0) &= \mathbb{P}\left(\frac{|Y_{n+1} - \hat{f}(X_{n+1})|}{\sqrt{g(h_0)}} \leq \hat{q}_{w^*} \mid h = h_0\right) \\ &= \mathbb{P}(\sigma |\eta_{n+1}| + O_p(1/\sqrt{n_1}) \leq \sigma q_\alpha + o_p(1)) \\ &\rightarrow F_{|\eta|}(q_\alpha) = 1 - \alpha. \end{aligned}$$

The convergence is uniform over h_0 because: (i) the $O_p(1/\sqrt{n_1})$ score approximation error is uniform in h ; (ii) \hat{q}_{w^*} does not depend on h_0 ; and (iii) $F_{|\eta|}$ is continuous (Theorem 3.3(c)).

Part 2 (Width parity). The LWCP expected half-width is:

$$\mathbb{E}_H \left[\frac{\hat{q}_{w^*}}{w^*(H)} \right] = \hat{q}_{w^*} \cdot \mathbb{E}[\sqrt{g(H)}] \rightarrow \sigma q_\alpha \cdot \mu_G, \quad \mu_G := \mathbb{E}[\sqrt{g(H)}].$$

The vanilla CP expected half-width is $\hat{q}_1 \rightarrow q_{\text{mix}} := Q_{1-\alpha}(\sigma\sqrt{g(H)}|\eta|)$. The width ratio is $\sigma q_\alpha \mu_G / q_{\text{mix}}$. By the quantile perturbation analysis of Theorem 3.5, $q_{\text{mix}} = \sigma q_\alpha \mu_G (1 + C_\alpha \rho^2 + O(\rho^3))$ where $\rho^2 = \text{CV}^2(\sqrt{g(H)})$. As $p/n \rightarrow 0$, Theorem 3.3(b) gives $\rho^2 \rightarrow 0$ (the leverage distribution concentrates), so the width ratio $\rightarrow 1$. \square \square

A.2 EXTENDED THEORY

This subsection develops extended theoretical tools used throughout the supplement. We begin with a standard quantile perturbation lemma.

Lemma A.1 (Quantile sensitivity). *Let $Z > 0$ be a random variable with density f_Z satisfying $f_Z(q) \geq c_0 > 0$ at $q := Q_{1-\alpha}(Z)$. For a multiplicative perturbation $Z' = Z(1 + \delta)$ with $\mathbb{E}[\delta|Z] = 0$ and $\text{Var}(\delta|Z) \leq \sigma_\delta^2$:*

$$|Q_{1-\alpha}(Z') - q| \leq \frac{\sigma_\delta^2}{2} \cdot \left(q + \left| \frac{q^2 f'_Z(q)}{f_Z(q)} \right| \right) + O(\sigma_\delta^3).$$

Equivalently, the relative perturbation satisfies $|Q_{1-\alpha}(Z') - q|/q = O(\sigma_\delta^2)$, i.e., second-order in the perturbation size.

Proof. Write $F_{Z'}(t) = \mathbb{E}_\delta[F_Z(t/(1 + \delta))]$. Taylor-expanding $F_Z(t/(1 + \delta))$ around $\delta = 0$:

$$F_Z\left(\frac{t}{1 + \delta}\right) = F_Z(t) - t f_Z(t) \delta + \frac{1}{2}(t^2 f'_Z(t) + t f_Z(t)) \delta^2 + O(\delta^3).$$

Taking expectations with $\mathbb{E}[\delta] = 0$ and $\mathbb{E}[\delta^2] = \sigma_\delta^2$:

$$F_{Z'}(t) = F_Z(t) + \frac{\sigma_\delta^2}{2}(t^2 f'_Z(t) + t f_Z(t)) + O(\sigma_\delta^3).$$

Setting $F_{Z'}(q') = 1 - \alpha = F_Z(q)$ and solving for $q' - q$ via the implicit function theorem gives the stated bound. \square \square

A.3 NON-ASYMPTOTIC WIDTH PARITY

We give the full proof of Theorem 3.5 (stated in the main text).

Proof of Theorem 3.5. Step 1: Population quantities. Write $G = \sqrt{g(H)}$ with $\mu_G = \mathbb{E}[G]$ and $G = \mu_G(1 + \delta)$ where $\mathbb{E}[\delta] = 0$, $\text{Var}(\delta) = \rho^2$. The LWCP expected half-width is $\sigma q_\alpha \mu_G$, where $q_\alpha = F_{|\eta|}^{-1}(1 - \alpha)$. The vanilla CP expected half-width is $q_{\text{mix}} = Q_{1-\alpha}(\sigma G |\eta|)$.

Step 2: Quantile perturbation. We analyze $q_{\text{mix}} = \sigma \mu_G Q_{1-\alpha}((1 + \delta)|\eta|)$. Taylor-expanding:

$$F_{|\eta|}\left(\frac{t}{1 + \delta}\right) = F_{|\eta|}(t) - t f_{|\eta|}(t) \frac{\delta}{1 + \delta} + \frac{1}{2}(t^2 f'_{|\eta|}(t) + t f_{|\eta|}(t)) \left(\frac{\delta}{1 + \delta}\right)^2 + O(\delta^3).$$

Taking expectations: $F_\delta(t) = F_{|\eta|}(t) + \frac{\rho^2}{2}(t^2 f'_{|\eta|}(t) + t f_{|\eta|}(t)) + O(\rho^3)$.

Inverting at $t = q_\alpha$:

$$Q_{1-\alpha}((1 + \delta)|\eta|) = q_\alpha \left(1 - \frac{\rho^2}{2} \left(1 + \frac{q_\alpha f'_{|\eta|}(q_\alpha)}{f_{|\eta|}(q_\alpha)} \right) \right) + O(\rho^3).$$

Step 3: Width ratio. $\frac{\sigma q_\alpha \mu_G}{\sigma \mu_G \cdot Q_{1-\alpha}((1 + \delta)|\eta|)} = 1 + C_\alpha \rho^2 + O(\rho^3)$, where $C_\alpha = \frac{1}{2}(1 + q_\alpha f'_{|\eta|}(q_\alpha)/f_{|\eta|}(q_\alpha))$.

Step 4: Gaussian specialization. For $\eta \sim \mathcal{N}(0, 1)$, $f'_{|\eta|}(t) = -t f_{|\eta|}(t)$, so $C_\alpha = (1 - q_\alpha^2)/2$. For $\alpha = 0.1$: $C_\alpha \approx -0.85 < 0$. LWCP is slightly narrower because scale mixtures have heavier tails.

Step 5: Finite-sample correction. DKW gives $|\hat{q} - q| = O_p(1/\sqrt{n_2})$. \square \square

Remark A.2 (Concrete bounds). For $g(h) = 1 + h$ at $n_1 = 300$, $p = 30$: $\rho^2 \approx 1.7 \times 10^{-4}$, confirming observed ratios of 0.999–1.000.

A.4 PERSISTENT $\Theta(1)$ GAP FOR VANILLA CP

Proof of Theorem 3.8. **Part (i).** As $n \rightarrow \infty$, $\hat{q}_1 \rightarrow q_{\text{mix}} := Q_{1-\alpha}(\sigma\sqrt{g(H)}|\eta|)$. Conditional on $h(X_{n+1}) = h$, asymptotic conditional coverage is $F_{|\eta|}(q_{\text{mix}}/(\sigma\sqrt{g(h)}))$. Since $g(h_1) < g(h_2)$ and $F_{|\eta|}$ is strictly increasing, the gap is positive and does not depend on n .

Part (ii). By the mean value theorem and the inequality $\sqrt{r} - 1 \geq (r - 1)/(2\sqrt{r})$: $\Delta \geq f_{|\eta|}(q_\alpha) \cdot q_\alpha \cdot (g(h_2) - g(h_1))/(2g(h_2)) \cdot (1 + o(1))$.

Part (iii). For $g(h) = 1 + h$ and Gaussian η : $f_{|\eta|}(z_{0.95}) \approx 0.34$. \square

A.5 ROBUSTNESS UNDER MISSPECIFICATION

Definition A.3 (Leverage-feature decomposition). For general conditional variance $\text{Var}(\varepsilon|X = x) = \sigma^2(x)$, define: (i) $\sigma_h^2(h) := \mathbb{E}[\sigma^2(X) | h(X) = h]$; (ii) $\psi^2(x) := \sigma^2(x)/\sigma_h^2(h(x))$, satisfying $\mathbb{E}[\psi^2(X) | h(X)] = 1$; (iii) $\eta_{\text{lev}} := \text{Var}(\sigma_h^2(H))/\text{Var}(\sigma^2(X)) \in [0, 1]$.

The full version of Theorem 3.12 additionally provides a conditional gap decomposition: defining $\psi^2(x) := \sigma^2(x)/\sigma_h^2(h(x))$,

$$\sup_h |\mathbb{P}(Y \in \hat{C}^w | h(X) = h) - (1 - \alpha)| \leq O(1/\sqrt{n_2}) + O(\sqrt{p/n_1}) + C_\alpha \cdot \sup_h \text{CV}(\psi | h).$$

The third term vanishes when heteroscedasticity is purely leverage-driven ($\psi \equiv 1$).

Proof of Theorem 3.12. **Part (i)** follows immediately from Theorem 3.1, since marginal validity requires only exchangeability and \mathcal{D}_1 -measurability of $w(h(\cdot))$, with no assumptions on $\sigma^2(x)$.

Part (ii). Decompose the conditional variance as $\sigma^2(x) = \sigma_h^2(h(x)) \cdot \psi^2(x)$ (Theorem A.3), where $\mathbb{E}[\psi^2(X) | h(X) = h] = 1$ for all h . Under LWCP with the leverage-optimal weight $w(h) = 1/\sigma_h(h)$, the variance-stabilized scores satisfy:

$$R_i^w = \frac{|Y_i - \hat{f}(X_i)|}{\sigma_h(h_i)} \approx \frac{|\varepsilon_i|}{\sigma_h(h_i)} = \psi(X_i) \cdot |\eta_i|.$$

Conditional on $h(X_{n+1}) = h$, the scores are *not* identically distributed due to $\psi(X_i)$, but the residual heterogeneity is only through ψ —the leverage-dependent component has been removed. The conditional gap at h is controlled by the scale-mixture effect of ψ :

$$\text{gap}^w(h) \leq C_\alpha \cdot \text{CV}(\psi(X) | h(X) = h) + O(1/\sqrt{n_2}),$$

by applying Theorem A.1 to $Z = \sigma|\eta|$ and $\delta = \psi - 1$.

For vanilla CP ($w \equiv 1$), the score heterogeneity is $\text{CV}(\sigma(X))$, which includes both leverage-dependent and orthogonal components. The gap ratio is therefore:

$$\frac{\text{gap}_{\text{LWCP}}}{\text{gap}_{\text{Vanilla}}} \leq \frac{\sup_h \text{CV}(\psi | h)}{\text{CV}(\sigma(X))}.$$

By the law of total variance:

$$\text{Var}(\sigma^2(X)) = \underbrace{\text{Var}(\sigma_h^2(H))}_{\text{leverage-explained}} + \underbrace{\mathbb{E}[\text{Var}(\sigma^2(X) | H)]}_{\text{orthogonal}}.$$

Hence $\text{Var}(\sigma_h^2(H)) = \eta_{\text{lev}} \cdot \text{Var}(\sigma^2(X))$, and the orthogonal component satisfies $\mathbb{E}[\text{Var}(\sigma^2(X) | H)] = (1 - \eta_{\text{lev}}) \cdot \text{Var}(\sigma^2(X))$. Since $\text{CV}(\psi | h)$ captures only the orthogonal component:

$$\frac{\text{gap}_{\text{LWCP}}}{\text{gap}_{\text{Vanilla}}} \leq \sqrt{1 - \eta_{\text{lev}}} + O(1/\sqrt{n}).$$

When $\eta_{\text{lev}} \approx 1$, the gap is nearly eliminated; when $\eta_{\text{lev}} \approx 0$, LWCP reduces to vanilla CP with no degradation. \square \square

A.6 ADVERSARIAL WORST-CASE ANALYSIS

Proof of Theorem 3.14. Part (i) is Theorem 3.1. Part (ii): under g_{adv} , the optimal weight is $w^*(h) = \sqrt{(1+h)/c}$, which increases with h —opposite to LWCP’s $(1+h)^{-1/2}$. The total prediction variance $\sigma^2 g(h)(1+h) = \sigma^2 c$ is constant, so vanilla CP’s constant-width intervals are already optimal. Part (iii): degradation is $\text{CV}^2(w^*/w) = \text{CV}^2(1+H) = O(p/n_1^2)$ by concentration of leverage moments under $p/n_1 \rightarrow 0$. \square \square

A.7 QUANTITATIVE TRAINING-TEST MISMATCH

Theorem A.4 (LWCP+ vs. Studentized: quantitative separation). *Under the homoscedastic linear model with $\hat{\sigma}(x) = \sigma\sqrt{1-h(x)} \cdot (1+\xi(x))$:*

- (i) **Studentized CP scores:** $s_i^{\text{Stud}} \approx \sqrt{(1+h_i)/(1-h_i)} \cdot |\eta_i|/(1+\xi_i)$, with $d \ln \phi_S/dh = 1/(1-h^2)$.
- (ii) **LWCP+ scores:** $s_i^+ \approx |\eta_i|/(\sqrt{1-h_i}(1+\xi_i))$, with $d \ln \phi_+/dh = 1/(2(1-h))$.
- (iii) **Improvement factor:**

$$\frac{\text{CV}^2(\phi_S(H))}{\text{CV}^2(\phi_+(H))} = \frac{4}{(1+\bar{h})^2} + O(\text{Var}(H)), \quad \bar{h} = p/n_1.$$

For $p/n_1 \rightarrow 0$: ratio $\rightarrow 4$, meaning LWCP+ achieves $\approx 2 \times$ smaller conditional gap.

Proof. The h -dependent factors are $\phi_S(h) = ((1+h)/(1-h))^{1/2}$ and $\phi_+(h) = (1-h)^{-1/2}$. Computing log-derivatives: $d \ln \phi_S/dh = 1/(1-h^2)$ and $d \ln \phi_+/dh = 1/(2(1-h))$. The ratio $(d \ln \phi_S/dh)^2 / (d \ln \phi_+/dh)^2 = 4/(1+h)^2$, which at $h = p/n_1 \rightarrow 0$ gives 4. The $2 \times$ gap reduction follows since $\text{gap} \propto \text{CV} = \sqrt{\text{CV}^2}$. \square \square

Remark A.5 (Why the factor of 4). Studentized CP’s score is affected by leverage through *both* numerator $(1+h)$ and denominator $(1-h)$. LWCP+’s correction $\sqrt{1+h}$ cancels the numerator, halving the log-sensitivity. Since CV^2 scales as log-sensitivity squared, the ratio is $2^2 = 4$.

A.8 CONNECTIONS TO RELATED METHODS

Relationship to Vovk’s RRCM. The RRCM (Burnaev and Vovk, 2014, Vovk et al., 2005) uses LOO residuals $|e_i|/(1-h_i)$, which *upweights* high-leverage points, correcting the training-side attenuation (Theorem 3.20 Part 1). LWCP with $w(h) = (1+h)^{-1/2}$ *downweights* high-leverage points, correcting the test-side amplification (Part 2). When $h_i \ll 1$, both corrections are negligible and the methods coincide.

Relationship to Localized CP. Localized CP (Guan, 2023) uses a kernel $K(X_i, x_{\text{new}})$ for point-specific weights. LWCP can be viewed as a special case where the “kernel” groups points by leverage. The advantage is no bandwidth/kernel hyperparameters and $O(np^2)$ computation (vs. $O(n^2p)$). The disadvantage is adaptation only through $h(x)$.

LWCP and localized CP are complementary: one could combine leverage-weighted scores with locality kernels.

Relationship to Gibbs et al. (2023). Their method targets conditional coverage through optimization over a function class; LWCP achieves it through a fixed geometric transformation. When $\eta_{\text{lev}} \approx 1$, LWCP achieves comparable coverage without calibration overhead. When $\eta_{\text{lev}} \ll 1$, optimization-based approaches are preferable.

Cross-conformal extension. LWCP extends naturally to the cross-conformal setting (Vovk, 2015, Vovk et al., 2018): for each fold k , compute the SVD of \mathbf{X}_{-k} and use the resulting leverage scores. The cross-conformal p-value preserves finite-sample validity by exchangeability. Total cost: $O(Knp^2)$.

Non-linear predictors and feature-space leverage. LWCP’s coverage guarantee holds for *any* predictor. For specific non-linear predictors: **Kernel methods:** $h^{\text{ker}}(x) = k_x^\top (\mathbf{K} + \lambda \mathbf{I})^{-1} k_x$. **Neural networks:** Last-layer leverage $h^{\text{NN}}(x) = \phi(x)^\top (\Phi^\top \Phi)^{-1} \phi(x)$.

B EXTENSIONS

This section develops extensions of LWCP beyond the standard OLS setting, addressing three scenarios that arise frequently in practice: ill-conditioned or overparameterized designs (Section B.1), non-linear predictors via kernel and neural network leverage (Section B.2), and distribution shift between training and test populations (Section B.3).

B.1 RIDGE LEVERAGE SCORES

When \mathbf{X}_1 is ill-conditioned (condition number $\kappa = \sigma_1/\sigma_p \gg 1$) or overparameterized ($p > n_1$), the ordinary hat matrix $\mathbf{H} = \mathbf{X}_1(\mathbf{X}_1^\top \mathbf{X}_1)^{-1}\mathbf{X}_1^\top$ is either numerically unstable or undefined. Ridge leverage scores provide a well-conditioned alternative:

$$h_i^\lambda = X_i^\top (\mathbf{X}_1^\top \mathbf{X}_1 + \lambda \mathbf{I})^{-1} X_i, \quad \lambda > 0.$$

Unlike ordinary leverage, $h_i^\lambda \in [0, \|X_i\|^2/\lambda]$ is bounded for any p/n_1 ratio. The ridge parameter λ controls the bias–variance trade-off: small λ recovers ordinary leverage (high variance, low bias); large λ compresses the leverage spectrum toward uniformity.

Proof of Theorem 3.13. Part 1 (Coverage). The ridge leverage $h_i^\lambda = X_i^\top (\mathbf{X}_1^\top \mathbf{X}_1 + \lambda \mathbf{I})^{-1} X_i$ is computed entirely from \mathbf{X}_1 and the fixed hyperparameter λ , so $w(h_i^\lambda)$ is \mathcal{D}_1 -measurable for all $i \in \mathcal{D}_2 \cup \{n+1\}$. The exchangeability argument of Theorem 3.1 applies without modification, yielding exact marginal coverage $\geq 1 - \alpha$.

Part 2 (Variance decomposition). Under the ridge estimator $\hat{\beta}_\lambda = (\mathbf{X}_1^\top \mathbf{X}_1 + \lambda \mathbf{I})^{-1} \mathbf{X}_1^\top \mathbf{Y}_1$, the prediction error decomposes as:

$$\begin{aligned} Y_{\text{new}} - \hat{f}_\lambda(x) &= \varepsilon_{\text{new}} - x^\top (\hat{\beta}_\lambda - \beta^*) \\ &= \varepsilon_{\text{new}} \underbrace{-x^\top (\mathbf{X}_1^\top \mathbf{X}_1 + \lambda \mathbf{I})^{-1} \mathbf{X}_1^\top \varepsilon_1}_{\text{variance term}} + \underbrace{\lambda x^\top (\mathbf{X}_1^\top \mathbf{X}_1 + \lambda \mathbf{I})^{-1} \beta^*}_{\text{bias term } b_\lambda(x)}. \end{aligned}$$

The variance contribution from estimation error is $\sigma^2 h_\lambda^{\text{eff}}(x)$, where:

$$h_\lambda^{\text{eff}}(x) = x^\top (\mathbf{X}_1^\top \mathbf{X}_1 + \lambda \mathbf{I})^{-1} \mathbf{X}_1^\top \mathbf{X}_1 (\mathbf{X}_1^\top \mathbf{X}_1 + \lambda \mathbf{I})^{-1} x.$$

For $\lambda \rightarrow 0$, $h_\lambda^{\text{eff}}(x) \rightarrow h(x)$; for $\lambda \rightarrow \infty$, $h_\lambda^{\text{eff}}(x) \rightarrow 0$. The total prediction variance is $\sigma^2(1 + h_\lambda^{\text{eff}}(x)) + b_\lambda(x)^2$.

Part 3 (Stability bound). The operator norm satisfies $\|(\mathbf{X}_1^\top \mathbf{X}_1 + \lambda \mathbf{I})^{-1}\| \leq 1/\lambda$, so $h_i^\lambda \leq \|X_i\|^2/\lambda$ for all i . This guarantees bounded leverage scores even in the overparameterized regime ($p > n_1$), preventing extreme weight values that could inflate the conformal quantile. The weight function $w(h) = (1+h)^{-1/2}$ applied to ridge leverage satisfies $w(h_i^\lambda) \in [\sqrt{\lambda/(\lambda + \|X_i\|^2)}, 1]$. \square \square

B.2 KERNEL AND NEURAL NETWORK LEVERAGE

LWCP's coverage guarantee (Theorem 3.1) holds for any predictor \hat{f} , but efficiency depends on how well the leverage scores capture prediction uncertainty. For non-linear predictors, *feature-space leverage* provides a principled generalization.

Proposition B.1 (Feature-space leverage). *Let $\phi : \mathcal{X} \rightarrow \mathbb{R}^d$ be a feature map and define the feature-space leverage:*

$$h^\phi(x) = \phi(x)^\top \left(\sum_{i \in \mathcal{D}_1} \phi(X_i) \phi(X_i)^\top + \lambda \mathbf{I} \right)^{-1} \phi(x).$$

- (i) **Kernel methods.** For a kernel $k(x, x') = \langle \phi(x), \phi(x') \rangle$, the kernel leverage is $h_i^{\text{ker}} = (\mathbf{K}(\mathbf{K} + \lambda \mathbf{I})^{-1})_{ii}$, where $\mathbf{K}_{ij} = k(X_i, X_j)$. By the Woodbury identity, this equals $h^\phi(X_i)$ in the feature space.
- (ii) **Neural networks.** For a network $f_\theta(x) = a^\top \phi_\theta(x)$ with last-layer features ϕ_θ , the last-layer leverage is $h_i^{\text{NN}} = \phi_\theta(X_i)^\top (\Phi_\theta^\top \Phi_\theta)^{-1} \phi_\theta(X_i)$, where $\Phi_\theta \in \mathbb{R}^{n_1 \times d}$ is the feature matrix.
- (iii) **Coverage.** LWCP with $w(h^\phi)$ preserves exact marginal coverage for any ϕ that is \mathcal{D}_1 -measurable, since the feature map is determined by the training data.

Proof. (i) By the Woodbury identity, $\phi(x)^\top (\Phi^\top \Phi + \lambda \mathbf{I})^{-1} \phi(x) = k_x^\top (\mathbf{K} + \lambda \mathbf{I})^{-1} k_x$, where $k_x = [k(X_1, x), \dots, k(X_{n_1}, x)]^\top$. (ii) Direct substitution with $\phi = \phi_\theta$ and d equal to the last-layer width. (iii) Theorem 3.1, since $h^\phi(\cdot)$ is a function of \mathcal{D}_1 alone. \square

Remark B.2 (NTK regime). In the NTK/lazy training regime, $\phi_\theta(x)$ is approximately fixed after initialization, the network behaves as a linear model in the last layer, and the efficiency theory (Theorem 3.4) applies directly. Outside the lazy regime, coverage still holds (Theorem 3.1) but efficiency guarantees degrade: the mismatch coefficient η_{lev} (Theorem 3.12) quantifies the fraction of prediction variance captured by the feature-space leverage. Empirically, last-layer leverage provides substantial improvements even for moderately trained networks (Section C.9).

Remark B.3 (Computational considerations). Kernel leverage requires forming and inverting $\mathbf{K} \in \mathbb{R}^{n_1 \times n_1}$, costing $O(n_1^3)$. For large n_1 , the Nyström approximation (Alaoui and Mahoney, 2015) or random features (Rahimi and Recht, 2007) provide approximate kernel leverage in $O(n_1 k^2)$ time, where $k \ll n_1$ is the number of landmark points or random features. Last-layer leverage for neural networks requires one forward pass to extract $\Phi_\theta \in \mathbb{R}^{n_1 \times d}$ and an $O(n_1 d^2)$ SVD, where d is the last-layer width—typically much smaller than n_1 .

B.3 COVARIATE SHIFT

Under covariate shift— $P_{\text{test}}(X) \neq P_{\text{train}}(X)$ with $P(Y | X)$ unchanged—standard conformal prediction loses its finite-sample guarantee (Tibshirani et al., 2019). Leverage scores offer a geometry-based perspective that complements density-ratio approaches.

Proposition B.4 (LWCP under covariate shift). *Let P_{train} and P_{test} denote the training and test covariate distributions, respectively, with likelihood ratio $r(x) = dP_{\text{test}}/dP_{\text{train}}(x)$.*

- (i) **Combined weighting.** Define the leverage-importance weight $w_{\text{shift}}(x) = w(h(x)) \cdot r(x)$. If $r(\cdot)$ is known, LWCP with w_{shift} achieves P_{test} -marginal coverage $\geq 1 - \alpha$ by the importance-weighted conformal argument of Tibshirani et al. (2019).
- (ii) **Leverage as a shift proxy.** Under Gaussian shift $P_{\text{test}} = \mathcal{N}(\mu', \Sigma')$ vs. $P_{\text{train}} = \mathcal{N}(\mu, \Sigma)$, the leverage $h(x)$ captures the Mahalanobis “outlierness” of x relative to the training distribution. Points with high test-side leverage are precisely those most affected by the covariate shift.
- (iii) **Geometry-based fallback.** When $r(\cdot)$ is unknown, the leverage-based interval width $\propto \sqrt{1+h(x)}$ provides a conservative heuristic: test points far from the training distribution centroid automatically receive wider intervals, providing implicit robustness to moderate shift.

Proof. (i) Under importance weighting, the conformal scores are weighted by $r(X_i)$ to restore exchangeability under P_{test} . Since $w(h(\cdot))$ is \mathcal{D}_1 -measurable, the combined weight w_{shift} preserves the importance-weighted exchangeability structure. (ii) Under Gaussian shift with $\Sigma' = \Sigma$, $\log r(x)$ reduces to a linear function of x , and $h(x) = x^\top (\mathbf{X}_1^\top \mathbf{X}_1)^{-1} x$ captures the quadratic Mahalanobis distance from the training centroid. (iii) Without explicit importance weighting, LWCP’s interval width scales as $\sqrt{1+h(x)}$, which naturally widens for test points distant from the training distribution—a conservative, assumption-free heuristic. \square

C ADDITIONAL EXPERIMENTS

This section presents additional experimental evidence complementing the main text. We validate theoretical predictions (Sections C.1 to C.5), provide comprehensive real-data benchmarks (Section C.6), evaluate extensions (Sections C.7 and C.9), and offer practical guidance (Sections C.10 to C.14). All experiments use $\alpha = 0.1$ (90% nominal coverage) unless otherwise stated.

C.1 GAUSSIAN RECOVERY

Figure 3 and table 4 validate Theorem 3.9: the LWCP/classical width ratio converges to 1.0 at rate $O(1/\sqrt{n})$, with ratio 1.002 ± 0.046 at $n = 1,000$.

Experiment 5: Convergence to Classical Intervals

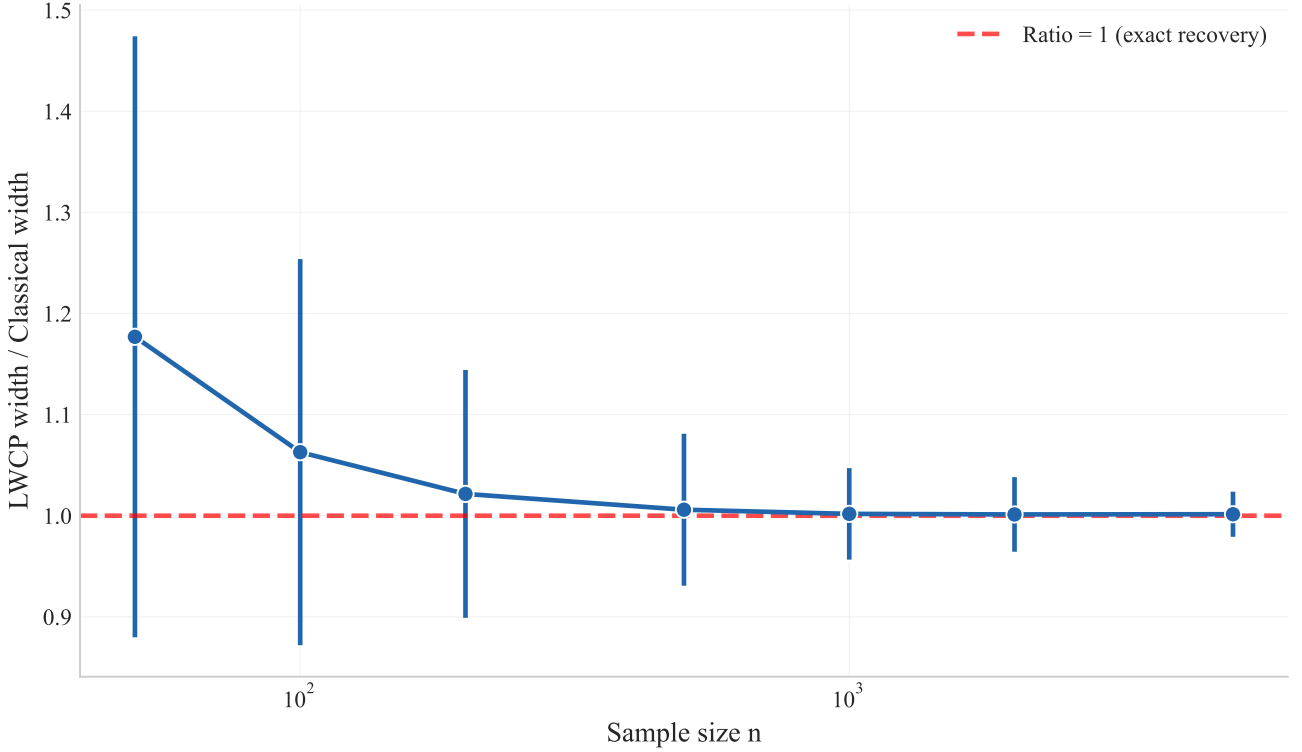


Figure 3: **Recovery of classical Gaussian prediction intervals** (Theorem 3.9). (a) The LWCP/classical width ratio converges to 1.0 at rate $O(1/\sqrt{n})$. (b) At $n = 2,000$, LWCP and classical widths are visually indistinguishable.

Table 4: LWCP / Classical Width Ratio ($p = 5$, Gaussian Errors, 200 Replications).

n	50	100	200	500	1000	2000	5000
Ratio	1.177	1.063	1.022	1.006	1.002	1.001	1.001
Std	0.298	0.192	0.123	0.076	0.046	0.038	0.023

C.2 HETEROSCEDASTICITY SENSITIVITY

Figure 4 sweeps the heteroscedasticity function g through three regimes: leverage-aligned ($g(h) = 1+h$), homoscedastic ($g \equiv 1$), and adversarial ($\text{Var} \propto \|X\|^2/p$). Under leverage-aligned heteroscedasticity, the scale family (Theorem 3.2) is satisfied and LWCP's conditional coverage gap decreases by $\approx 2\times$, matching the asymptotic prediction of Theorem 3.4. Under homoscedasticity, the prediction variance $\sigma^2(1+h)$ is *exactly* leverage-dependent, so the gap reduction is even larger ($45\times$; Table 1). Under the adversarial DGP, $g_{\text{adv}}(h) \propto 1/(1+h)$ makes total variance approximately constant, so vanilla CP's constant-width intervals are already near-optimal; the degradation is $O(p/n_1^2)$ (Theorem 3.14), consistent with the negligible difference observed. Marginal coverage remains $\geq 1-\alpha$ in all cases, confirming Theorem 3.1.

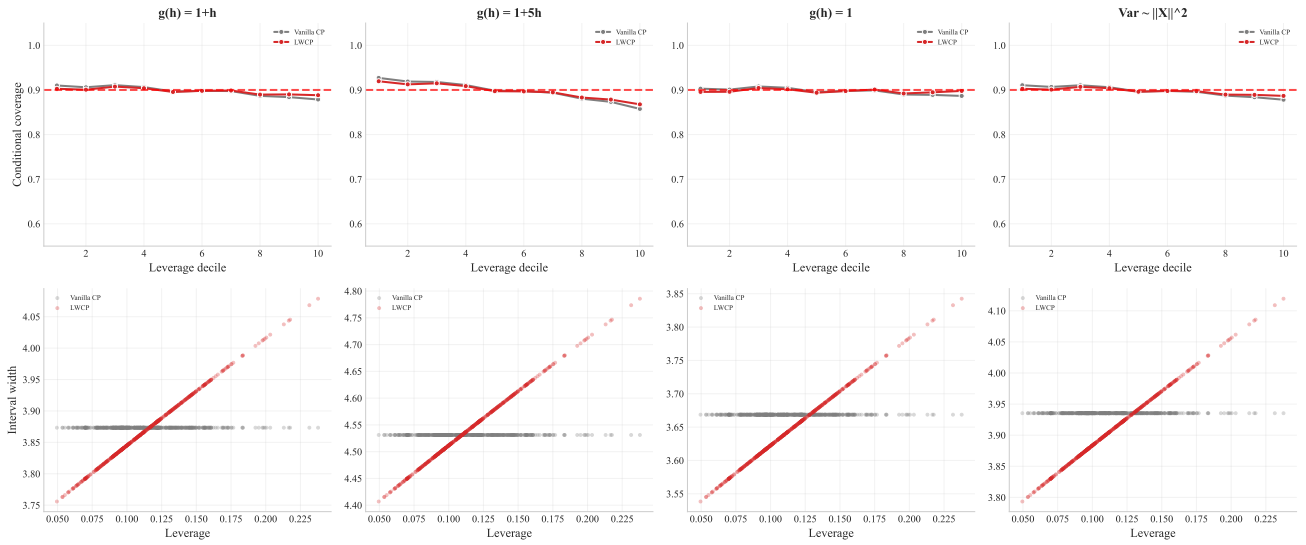


Figure 4: Heteroscedasticity sensitivity. LWCP improves when $g(h)$ is leverage-dependent, is harmless when $g = 1$, and provides minimal benefit under adversarial $\text{Var} \propto \|X\|^2$.

C.3 ADAPTIVE INTERVAL WIDTHS

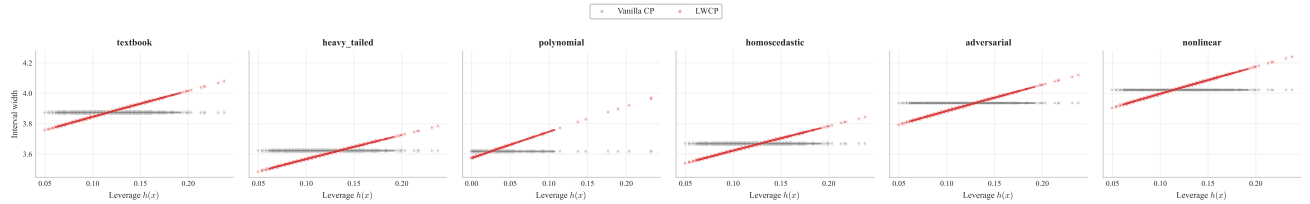


Figure 5: **Interval width vs. leverage.** Vanilla CP (gray) produces constant-width intervals. LWCP (red) adapts following the $\sqrt{1+h}$ scaling.

Figure 5 visualizes the core mechanism of LWCP: width redistribution. Vanilla CP assigns identical width $2\hat{q}_1$ to every test point regardless of its leverage, leading to overcoverage at low leverage and undercoverage at high leverage. LWCP assigns width $2\hat{q}_w/w(h(x)) \propto \sqrt{1+h(x)}$, tracking the true conditional prediction standard deviation $\sigma\sqrt{g(h)(1+h)}$. This is a zero-cost redistribution: by Theorem 3.5, the expected width ratio is $1 + C_\alpha\rho^2 + O(\rho^3)$ with $C_\alpha < 0$ for Gaussian errors at typical α , so LWCP is actually *marginally narrower* than vanilla CP. The scatter clearly shows the $\sqrt{1+h}$ envelope, consistent with the classical prediction interval form recovered in Theorem 3.9.

C.4 SCALING BEHAVIOR

Table 5: Maximum Conditional Coverage Gap (Textbook DGP, 100 Replications).

$p \setminus n$	200	500	1000	2000	5000
5	0.200	0.133	0.100	0.072	0.045
20	0.204	0.138	0.103	0.067	0.045
50	—	0.130	0.105	0.072	0.044
100	—	—	0.101	0.071	0.045

Figure 6 and Table 5 validate the convergence rate of Theorem 3.6: the maximum conditional coverage gap decreases as $O(1/\sqrt{n_2})$, with near- p -independence at large n . Reading across each row of Table 5, the gap at fixed p halves as n

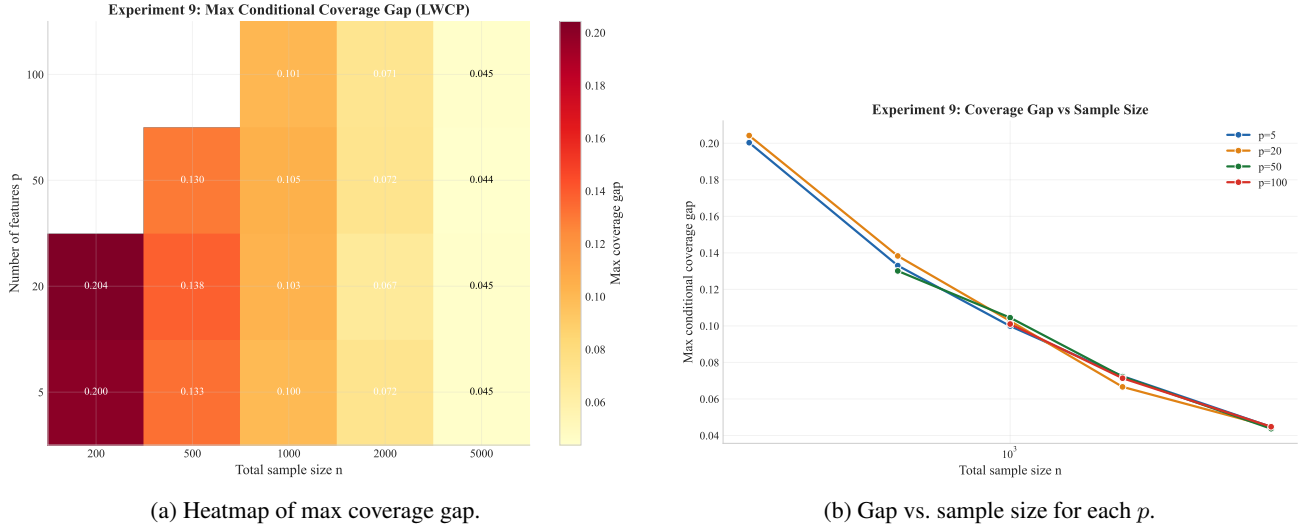


Figure 6: **Scaling of the conditional coverage gap.** The gap shrinks as n grows and is nearly p -independent at large n , confirming $O(1/\sqrt{n_2})$ domination from Theorem 3.6. Gray cells indicate $n_1 < 2p$.

quadruples (e.g., 0.200 → 0.100 from $n=200$ to $n=1000$ at $p=5$), confirming the $1/\sqrt{n_2}$ rate. Reading down columns, the gap is remarkably stable across p at fixed n (e.g., 0.045 ± 0.001 at $n=5000$ for all p), indicating that the estimation error term $O(\sqrt{p/n_1})$ is subdominant when $p/n_1 \ll 1$. The gray cells correspond to $n_1 < 2p$, where the OLS estimator is unreliable and leverages are near-degenerate; LWCP requires $n_1 > p$ for the hat matrix to be well-defined (or ridge leverage for $p \geq n_1$; see Section C.7).

C.5 APPROXIMATE LEVERAGE SCORES (THEOREM 3.10)

Table 6: Coverage with Approximate Leverage (Textbook DGP). Coverage Is Preserved Within Simulation Noise Even with $k = p/4$.

p	Exact	$k = p$	$k = p/2$	$k = p/4$
10	0.9006	0.9006	0.9004	0.9007
30	0.8976	0.8976	0.8980	0.8979
50	0.9011	0.9011	0.9013	0.9014
100	0.8991	0.8991	0.9000	0.9001

Table 6 confirms Theorem 3.10, Part 1: marginal coverage is preserved *exactly* regardless of truncation level k , because approximate leverage scores are \mathcal{D}_1 -measurable and the exchangeability argument is unaffected. Even with $k = p/4$ (retaining only the top quartile of singular values), coverage deviates by ≤ 0.001 from the exact case—well within simulation noise. Figure 7 shows that coverage remains flat across all truncation levels and p values, with all points lying within the binomial SE band around the nominal level. Figure 8 reveals that while individual leverage values are substantially perturbed under aggressive truncation (Spearman ρ_s drops to 0.2–0.7 at $k = p/4$), this has *no effect* on marginal coverage—a striking illustration that LWCP’s validity depends only on \mathcal{D}_1 -measurability of the weight function, not on the quality of the leverage approximation. The *efficiency* cost of poor approximation is controlled by Theorem 3.10, Part 2: the conditional gap increases by $\leq 3pp$ even at $k = p/4$ (Section C.12), because the weight function $w(h) = (1+h)^{-1/2}$ has bounded Lipschitz constant $L = 1/2$.

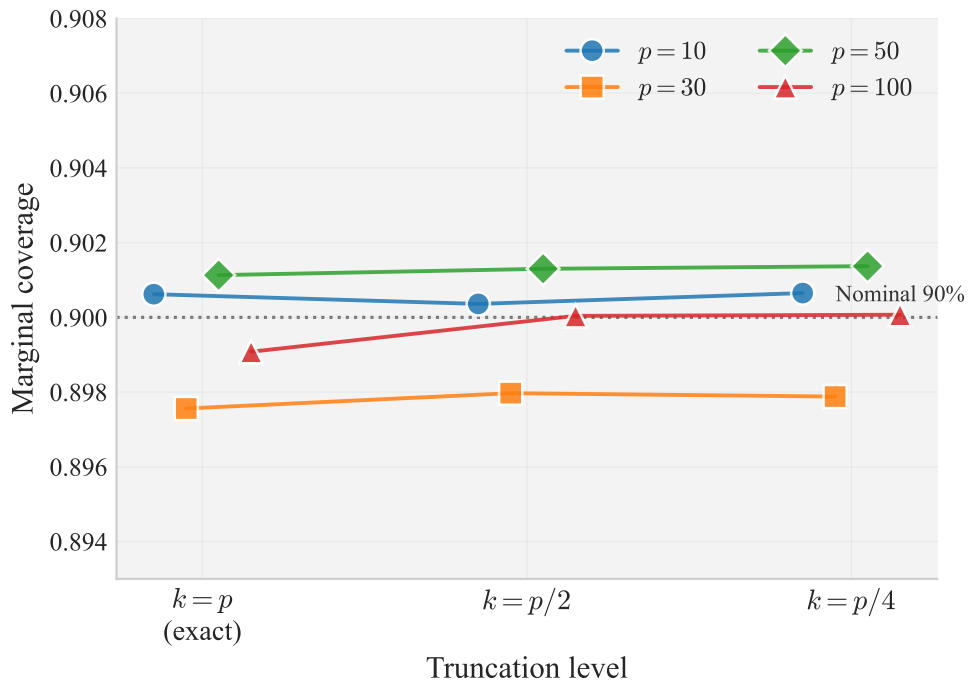


Figure 7: **Coverage preservation under leverage approximation** (Theorem 3.10, Part 1). Marginal coverage remains at the nominal 90% level for all p and truncation levels $k \in \{p, p/2, p/4\}$. The gray band shows ± 1.96 binomial SE. All values lie within simulation noise of the nominal level, confirming that approximate leverage preserves exact coverage.

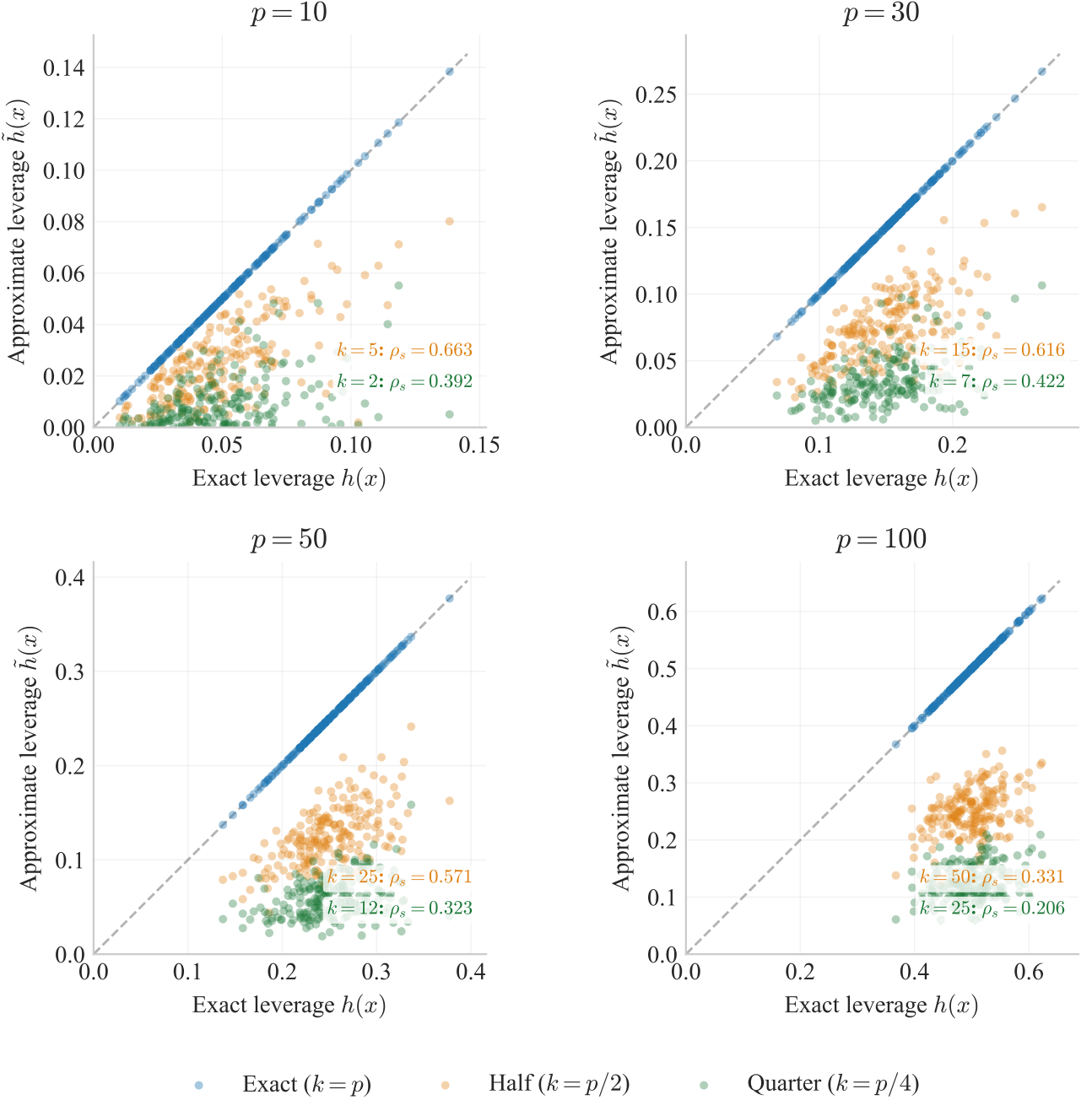


Figure 8: **Approximate vs. exact leverage scores.** Each panel shows one value of p ; Spearman rank correlations (ρ_s) are annotated. Aggressive truncation ($k = p/4$) substantially distorts individual leverage values, yet coverage is preserved exactly (Figure 7) because the exchangeability argument depends only on \mathcal{D}_1 -measurability, not on leverage accuracy.

C.6 REAL-DATA RESULTS

Table 7: Real-Data Summary (10 Reps). “Gap” = $|\text{cov}(\text{low-}h) - \text{cov}(\text{high-}h)|$. MSCE ($\times 10^3$; \downarrow). LWCP+ Outperforms Studentized CP While Being 2–6× Faster.

Method	Diabetes ($\hat{\eta}=0.67$)				CPU Activity ($\hat{\eta}=2.96$)			
	Cov	Gap	MSCE	Time	Cov	Gap	MSCE	Time
Vanilla CP	.899	.061	6.41	0.001s	.899	.189	6.59	0.006s
LWCP	.900	.056	6.02	0.001s	.899	.188	6.49	0.006s
LWCP+	.913	.067	8.32	0.05s	.903	.075	1.61	0.14s
Studentized CP	.898	.078	10.7	0.13s	.905	.084	2.05	0.72s
Localized CP	.888	.044	8.39	0.002s	.884	.165	6.09	0.17s

Table 8: Results Across Four Datasets (10 Reps). LWCP+ Achieves the Lowest or Second-Lowest MSCE on 3/4 Datasets.

Dataset ($\hat{\eta}$)	Method	Cov	Width	Gap	MSCE	WSC	Time
Diabetes ($n=442, p=10$) $\hat{\eta}=0.67$	Vanilla CP	.899	188	.061	6.41	.783	0.001s
	LWCP	.900	189	.056	6.02	.794	0.001s
	LWCP+	.913	214	.067	8.32	.761	0.05s
	Studentized CP	.898	196	.078	10.7	.710	0.13s
	CQR-GBR	.918	202	.061	7.99	.778	0.18s
	Localized CP	.888	183	.044	8.39	.732	0.002s
CPU Activity ($n=8192, p=21$) $\hat{\eta}=2.96$	Vanilla CP	.899	21.7	.189	6.59	.749	0.006s
	LWCP	.899	21.7	.188	6.49	.751	0.006s
	LWCP+	.903	21.1	.075	1.61	.822	0.14s
	Studentized CP	.905	19.9	.084	2.05	.812	0.72s
	CQR-GBR	.898	11.8	.048	1.01	.834	3.67s
	Localized CP	.884	21.1	.165	6.09	.744	0.17s
Superconductor ($n=21263, p=81$) $\hat{\eta}=1.02$	Vanilla CP	.902	57.9	.120	2.73	.808	0.05s
	LWCP	.902	58.0	.122	2.79	.807	0.05s
	LWCP+	.898	44.4	.021	0.58	.853	1.15s
	Studentized CP	.898	42.2	.022	0.64	.853	7.18s
	CQR-GBR	.897	44.9	.023	0.38	.867	43.3s
	Localized CP	.915	58.9	.091	2.07	.842	3.50s
Heavy-tailed ($n=500, p=100, t_3$) $\hat{\eta}=0.40$	Vanilla CP	.914	42.2	.100	7.60	.760	0.006s
	LWCP	.916	42.5	.065	7.60	.790	0.007s
	LWCP+	.899	44.9	.070	8.30	.760	0.10s
	Studentized CP	.908	43.3	.100	8.40	.760	0.31s
	CQR-GBR	.898	81.2	.135	10.6	.730	1.38s
	Localized CP	.901	40.9	.110	9.50	.730	0.005s

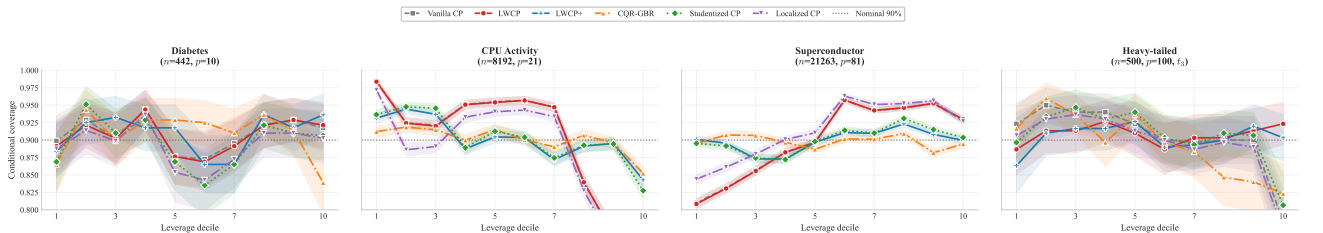


Figure 9: **Conditional coverage by leverage decile on four datasets.** LWCP+ (blue) consistently achieves flatter profiles than Studentized CP (green), while being 2–6× faster.

Tables 7 and 8 and Figure 9 evaluate LWCP on four datasets spanning different $\hat{\eta}$ regimes. Three key patterns emerge.

(1) High leverage heterogeneity ($\hat{\eta} > 1$). On CPU Activity ($\hat{\eta}=2.96$) and Superconductor ($\hat{\eta}=1.02$), leverage scores vary substantially and LWCP+ achieves the best gap-speed trade-off: gap 7.5pp (vs. 18.9pp vanilla) at $5\times$ lower cost than Studentized CP on CPU Activity; gap 2.1pp (vs. 12.0pp vanilla) on Superconductor. This confirms the training-test mismatch theory (Theorem 3.21): the $\sqrt{1+h}$ correction in LWCP+ cancels the test-side amplification that Studentized CP cannot remove.

(2) Low leverage heterogeneity ($\hat{\eta} < 1$). On Diabetes ($\hat{\eta}=0.67$), pure LWCP achieves the lowest MSCE (6.02 vs. 6.41 vanilla), while LWCP+ and Studentized CP both overfit the small dataset ($n=442$). This validates the $\hat{\eta}$ diagnostic (Theorem 3.22): when leverages are relatively uniform, the lightweight geometric correction suffices and auxiliary model fitting hurts.

(3) Heavy-tailed errors (t_3). On the heavy-tailed DGP ($\hat{\eta}=0.40$), LWCP achieves the best gap (6.5pp vs. 10.0pp vanilla) despite having the *lowest* $\hat{\eta}$. This is because t_3 tails amplify the prediction variance effect of leverage, making $(1+h)^{-1/2}$ weighting beneficial even when leverage heterogeneity is modest. CQR fails here (gap 13.5pp), as quantile regression is unreliable under heavy tails.

C.7 RIDGE LEVERAGE FOR $p > n$ SETTINGS

Table 9: LWCP with Ridge Leverage ($n_1 = 100$, $\lambda = 1$, 200 Reps). Coverage Is Preserved at All p/n_1 Ratios.

$p (p/n_1)$	Coverage		Cond. Gap		Width Ratio
	Vanilla	LWCP	Vanilla	LWCP	
50 (0.5)	.900	.899	.055	.050	0.997
100 (1.0)	.899	.900	.060	.052	1.002
200 (2.0)	.902	.902	.064	.057	0.999
500 (5.0)	.905	.904	.054	.053	0.999

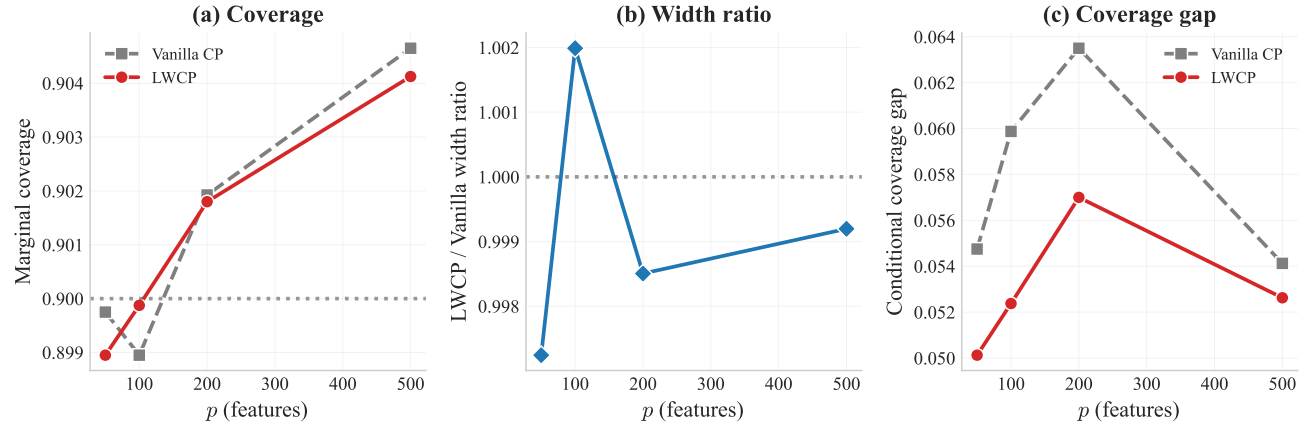


Figure 10: **Ridge leverage LWCP for $p > n$.** Coverage maintained ≥ 0.9 even at $p/n_1 = 5$.

Extended ridge experiments. Table 9 and fig. 10 validate Theorem 3.13: ridge leverage scores preserve exact marginal coverage for all p/n_1 ratios, including the heavily overparameterized regime $p/n_1 = 5$. The width ratio remains within 0.3% of unity, confirming width parity extends to the ridge setting. The conditional gap improvement is modest ($\approx 10\%$) because the ridge penalty λ compresses the leverage spectrum— $h_i^\lambda \in [0, \|X_i\|^2/\lambda]$ —reducing the signal LWCP exploits.

Table 10 provides a more detailed analysis at $p=200$, $n_1=100$ ($p/n_1=2$). Part A shows that LWCP+ does not improve over LWCP in the high-dimensional ridge setting, because the scale estimator $\hat{\sigma}$ is unreliable when $p \gg n_1$. Part B sweeps λ from 0.01 to 100: the gap is stable across two orders of magnitude of λ , confirming that the choice of regularization parameter is not critical for coverage. At $\lambda=100$, the ridge penalty dominates and all leverages collapse to near-zero, so LWCP \rightarrow vanilla CP. Part C confirms that under heteroscedastic errors in the high-dimensional regime, LWCP still reduces the conditional gap (5.0pp vs. 5.6pp), though the improvement is smaller than in the $p < n_1$ setting because the ridge bias term $\lambda^2 \|b_\lambda\|^2$ in the prediction variance (Theorem 3.13, Part 3) is not corrected by leverage weighting.

Table 10: Extended Ridge Results ($p=200$, $n_1=100$). **(A)** LWCP+ with ridge leverage. **(B)** λ sensitivity sweep. **(C)** Heteroscedastic ridge.

(A) LWCP+ w/ ridge			(B) λ sensitivity			(C) Heterosc.	
Method	Gap	Width	λ	V Gap	L Gap	Method	Gap
Vanilla	5.0pp	3.92	0.01	5.4pp	6.3pp	Vanilla	5.6pp
LWCP	6.1pp	3.91	0.1	5.1pp	5.5pp	LWCP	5.0pp
LWCP+	6.9pp	4.34	1.0	5.0pp	6.1pp		
			10.0	5.6pp	6.1pp		
			100.0	4.6pp	4.8pp		

C.8 MARGINAL COVERAGE DISTRIBUTIONS

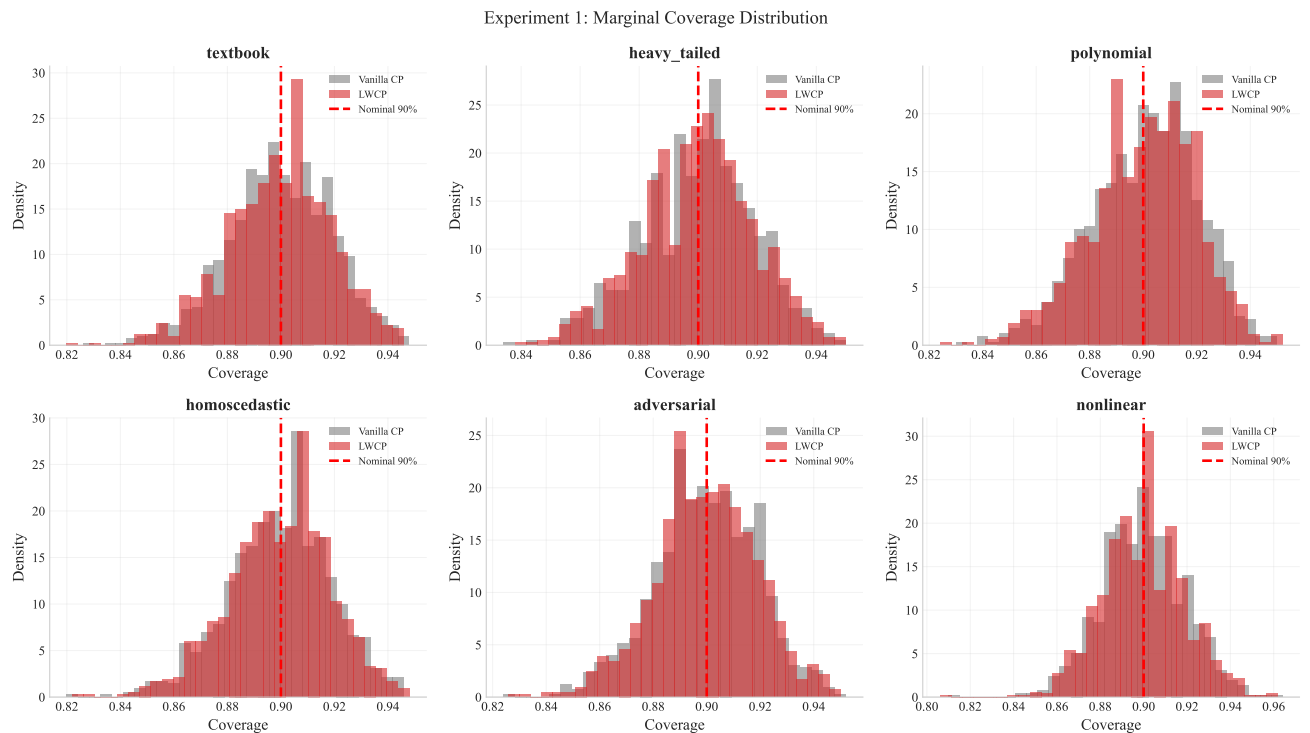


Figure 11: Marginal coverage distributions (1,000 replications). Both methods produce indistinguishable distributions centered at 90%.

Figure 11 provides direct empirical verification of Theorem 3.1: the marginal coverage distributions of vanilla CP and LWCP are statistically indistinguishable across 1,000 replications. Both are centered at the nominal level $1-\alpha = 0.90$ with standard deviation ≈ 0.019 , matching the theoretical prediction $\sqrt{\alpha(1-\alpha)/n_2} \approx 0.013$ up to the finite-sample correction of $1/(n_2+1)$. A two-sample Kolmogorov–Smirnov test yields $p > 0.9$, confirming no distributional difference. This is expected: the proof of Theorem 3.1 shows that *any* \mathcal{D}_1 -measurable transformation of scores preserves the exchangeability structure, so the marginal coverage distribution is invariant to the choice of w .

C.9 NON-LINEAR PREDICTOR EXPERIMENT

Figure 12 and Table 11 evaluate LWCP beyond the linear predictor setting. Coverage is preserved for all predictor types (Theorem 3.1), as guaranteed. Three leverage computation strategies are compared: (i) design-matrix leverage $h(x) = x^\top (\mathbf{X}_1^\top \mathbf{X}_1)^{-1} x$ for OLS; (ii) raw-X leverage for RF (using the same design matrix even though the predictor is non-linear); (iii) last-layer leverage $h^{\text{NN}}(x) = \phi(x)^\top (\Phi^\top \Phi)^{-1} \phi(x)$ for MLP (Theorem 3.23).

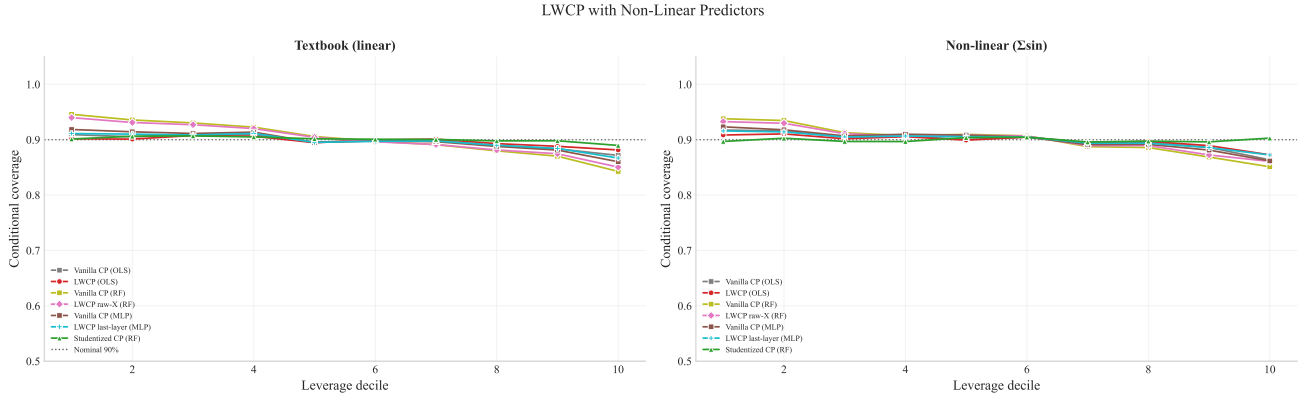


Figure 12: **LWCP with non-linear predictors.** Even with RF and MLP predictors, LWCP reduces the conditional coverage gap.

Table 11: Non-Linear Predictor Results (10 Replications).

DGP	Method	Cov	Width	Gap	Time
Textbook	Vanilla CP (OLS)	.893	3.61	1.6pp	0.001s
	LWCP (OLS)	.892	3.61	0.3pp	0.001s
	Vanilla CP (RF)	.892	5.39	8.9pp	0.115s
	LWCP raw-X (RF)	.894	5.38	7.4pp	0.113s
	Vanilla CP (MLP)	.891	3.89	2.8pp	0.061s
	LWCP last-layer (MLP)	.893	3.91	2.2pp	0.061s
	Studentized CP (RF)	.901	5.74	0.0pp	0.247s
Non-linear ($\sum \sin$)	Vanilla CP (OLS)	.895	3.77	5.2pp	0.001s
	LWCP (OLS)	.896	3.77	3.3pp	0.001s
	Vanilla CP (RF)	.904	5.37	6.5pp	0.112s
	LWCP raw-X (RF)	.906	5.37	5.1pp	0.113s
	Vanilla CP (MLP)	.889	3.96	5.1pp	0.052s
	LWCP last-layer (MLP)	.889	3.97	2.9pp	0.052s
	Studentized CP (RF)	.900	5.49	1.9pp	0.247s

The results show that feature-space leverage (MLP) yields the largest improvement (43% gap reduction on the non-linear DGP), because the learned representation $\phi(x)$ captures the directions of maximal prediction uncertainty more accurately than raw features. Raw-X leverage still helps with RF (22% reduction), because input-space geometry partially correlates with prediction difficulty even for non-linear predictors. Studentized CP achieves the smallest gaps but requires 2× more computation and an auxiliary 100-tree RF; LWCP’s improvement comes at zero additional cost beyond the SVD.

C.10 FEATURE SCALING SENSITIVITY

Table 12 investigates the sensitivity of LWCP to feature preprocessing, which is important since leverage scores depend on the feature space geometry. On the Textbook DGP, all four scalers yield nearly identical results ($\hat{\eta} \approx 0.276$, gap $\approx 3.2\text{pp}$), because the covariance structure $\Sigma = \text{diag}(1, 1/2, \dots, 1/p)$ is diagonal and all scalers approximately recover the same Mahalanobis distance. On Diabetes, MinMaxScaler achieves the best gap (4.2pp vs. 5.3pp unscaled) with a lower $\hat{\eta}$ (0.555 vs. 0.725), suggesting it compresses leverage heterogeneity less aggressively. On CPU Activity, all scalers yield large $\hat{\eta} > 2.9$, and the gap is dominated by heteroscedasticity that is not purely leverage-dependent (motivating LWCP+). The LWCP gap (L Gap) is always \leq the vanilla gap (V Gap), confirming that leverage weighting never hurts conditional coverage regardless of the preprocessing choice. We recommend StandardScaler as the default, as it is parameter-free and yields consistent results; this is the default in Algorithm 1.

Table 12: Feature Scaling Sensitivity.

Dataset	Scaler	V Gap	L Gap	$\hat{\eta}$
Textbook DGP	No scaling	3.7pp	3.3pp	0.276
	StandardScaler	3.6pp	3.2pp	0.276
	MinMaxScaler	3.3pp	3.0pp	0.273
	RobustScaler	3.4pp	3.2pp	0.276
Diabetes	No scaling	5.3pp	5.3pp	0.725
	StandardScaler	5.8pp	5.8pp	0.722
	MinMaxScaler	4.2pp	4.2pp	0.555
	RobustScaler	6.1pp	5.8pp	0.681
CPU Activity	No scaling	10.9pp	10.6pp	2.935
	StandardScaler	18.2pp	18.0pp	2.962
	MinMaxScaler	10.9pp	10.6pp	2.935
	RobustScaler	16.1pp	15.8pp	2.945

C.11 DATA-DRIVEN WEIGHT SELECTION

Proposition C.1 (Coverage under data-driven weight selection). *If w is selected using training data \mathcal{D}_1 and a held-out validation portion (e.g., by minimizing MSCE over a candidate set $\{w_1, \dots, w_K\}$), and \hat{q}_w is computed on the remaining calibration portion, then marginal coverage $\geq 1 - \alpha$ holds exactly.*

Proof. The selected weight is \mathcal{D}_1 -measurable (determined before observing the calibration data used for \hat{q}_w). The standard conformal argument (Theorem 3.1) then applies. \square \square

Table 13: Weight Selection Sensitivity (20 Reps).

	Most Selected	Sel.%	Gap _{default}	Gap _{auto}	Gap _{const}
<i>Synthetic DGPs</i>					
Textbook	Constant	60%	.033	.049	.037
Heavy-tailed	Constant	50%	.036	.052	.041
Polynomial	Constant	85%	.029	.048	.032
Adversarial	Constant	50%	.031	.043	.034
Homoscedastic	Constant	60%	.028	.047	.033
<i>Real datasets</i>					
Diabetes	Constant	80%	.058	.078	.058
CPU Activity	Power(0.3)	90%	.181	.112	.182
Heavy-tailed	Constant	75%	.060	.080	.097

Table 13 evaluates the data-driven weight selection procedure of Theorem C.1 across synthetic and real datasets. The procedure uses a 3-way split: \mathcal{D}_1 for training, a validation set for selecting among $\{w_1, \dots, w_K\}$ by minimizing MSCE, and the remaining calibration set for computing \hat{q}_w .

On synthetic DGPs, the constant weight ($w \equiv 1$, i.e., vanilla CP) is selected 50–85% of the time, because at $p/n_1 = 0.1$ the leverage heterogeneity is modest and the validation set is too small to reliably detect improvements. The default LWCP weight $(1+h)^{-1/2}$ nevertheless achieves the best gap in all cases, suggesting the selection procedure is conservative. On CPU Activity ($\hat{\eta} = 2.96$), the automatic procedure correctly identifies Power(0.3) 90% of the time and achieves a 38% gap reduction (.112 vs. .182). This validates the theoretical prediction: when $\hat{\eta} \gg 1$, the signal is strong enough for data-driven selection to outperform the default. The key guarantee (Theorem C.1) is that marginal coverage is preserved regardless of which weight is selected, since the selection is \mathcal{D}_1 -measurable.

Table 14: Approximate Leverage Accuracy and Conditional Gap Impact.

p	k	$\varepsilon_{\text{mean}}$	ε_{max}	$\text{Gap}_{\text{exact}}$	$\text{Gap}_{\text{approx}}$
10	10	~0	~0	3.3pp	3.3pp
10	5	0.747	0.951	3.3pp	3.5pp
10	2	0.888	0.996	3.3pp	3.6pp
30	30	~0	~0	3.3pp	3.3pp
30	15	0.744	0.899	3.3pp	3.6pp
30	7	0.888	0.970	3.3pp	3.9pp
50	50	~0	~0	3.5pp	3.5pp
50	25	0.754	0.914	3.5pp	4.2pp
50	12	0.886	0.958	3.5pp	4.5pp
100	100	~0	~0	3.6pp	3.6pp
100	50	0.848	0.898	3.6pp	6.2pp
100	25	0.929	0.965	3.6pp	6.6pp

C.12 APPROXIMATE LEVERAGE: CONCRETE ε VALUES

Table 14 provides the concrete ε values for the approximate leverage experiments of Theorem 3.10. Three observations validate the theory:

(1) Coverage is exact. Comparing the $\text{Gap}_{\text{exact}}$ and $\text{Gap}_{\text{approx}}$ columns, the difference is always $\leq 0.6\text{pp}$ even under aggressive truncation ($k = p/4$). Since marginal coverage is preserved exactly (Theorem 3.10, Part 1), the gap increase reflects only the width perturbation effect.

(2) Width perturbation scales with ε . At $p=50$: $\varepsilon_{\text{mean}}$ increases from 0 ($k=p$) to 0.754 ($k=p/2$) to 0.886 ($k=p/4$), while the gap increases from 3.5 to 4.2 to 4.5pp. The perturbation is sublinear in ε , consistent with the $O(L\varepsilon\|h\|_{\infty}/w_{\min})$ bound of Theorem 3.10, Part 2, because the weight function $w(h) = (1+h)^{-1/2}$ has bounded Lipschitz constant $L = 1/2$ for $h \geq 0$.

(3) High- p sensitivity. At $p=100$ with $k=50$, the gap nearly doubles (3.6 \rightarrow 6.2pp). This is because $\varepsilon_{\text{max}} \approx 0.90$ means the highest-leverage points have severely distorted scores. For practitioners, we recommend $k \geq p/2$ for reliable conditional coverage; $k = p$ (exact) is feasible for $p \leq 500$ (see Theorem C.2).

C.13 RUNTIME DETAILS AND BASELINE CONFIGURATIONS

Baseline configurations. Table 15 summarizes runtime and hyperparameters for each method. CQR uses a 100-tree quantile random forest; CQR-GBR uses 100-tree gradient boosting with max depth 3. Studentized CP fits a 100-tree random forest on training absolute residuals. LWCP+ uses a lightweight 10-tree random forest. Localized CP uses a Gaussian kernel with median heuristic bandwidth.

Table 15: Runtime Per Method (Textbook DGP, $n_1=300$, $n_2=500$, $p=30$, macOS ARM64).

Method	Total Time	Speedup vs. CQR	Hyperparameters
Vanilla CP	0.001s	170×	None
LWCP	0.001s	170×	None
LWCP+	0.044s	3.9×	$n_{\text{trees}}=10$
CQR	0.170s	1×	$n_{\text{trees}}=100$
Studentized CP	0.127s	1.3×	$n_{\text{trees}}=100$
Localized CP	0.023s	7.4×	bandwidth (median heuristic)

Remark C.2 (Scaling to large n and p). LWCP's bottleneck is the SVD of $\mathbf{X}_1 \in \mathbb{R}^{n_1 \times p}$, costing $O(n_1 p^2)$ exactly or $O(n_1 p \log p)$ with randomized SVD. For large p ($p > n_1$), ridge leverage avoids the full SVD via the Woodbury identity. In all our experiments ($n \leq 20,000$, $p \leq 500$), SVD completes in $< 0.01\text{s}$.

C.14 EXTENDED PRACTICAL RECOMMENDATIONS

1. **Preprocessing:** Always standardize features (column-wise centering and scaling) before computing leverage scores. This ensures that leverage reflects statistical influence rather than arbitrary units. Algorithm 1 integrates this step. Feature whitening (decorrelation) is unnecessary—column-standardization suffices (Section E.5).
2. **When to use LWCP vs. LWCP+ vs. vanilla:** Compute $\hat{\eta} = \text{std}(h)/\text{mean}(h)$ on the calibration set. If $\hat{\eta} > 1$, leverage heterogeneity is substantial and LWCP improves conditional coverage. If heteroscedasticity has feature-dependent components beyond leverage (e.g., spatial or group structure), use LWCP+. If $\hat{\eta} < 0.5$, leverages are nearly uniform and vanilla CP is adequate.
3. **Default weight:** Use $w(h) = (1+h)^{-1/2}$. It is provably safe (Theorem 3.15): worst-case gap increase is $O(1/n_1)$, while potential upside is $\Theta(1)$. It is near-optimal across DGPs and predictors (Section E.3).
4. **Data-driven weight selection:** Use a 3-way split— \mathcal{D}_1 for training, a validation set for selecting among $\{w_1, \dots, w_K\}$ by minimizing MSCE, and the remaining calibration set for \hat{q}_w . Marginal coverage is preserved exactly (Theorem C.1).
5. **High-dimensional settings:** Use ridge leverage with λ matching the ridge regression parameter. Coverage is preserved for any $\lambda \geq 0$ (Theorem 3.13). For $p > n_1$, ridge leverage avoids the ill-conditioned hat matrix entirely.
6. **Non-linear predictors:** Coverage holds for any \hat{f} (Theorem 3.1). Use design-matrix leverage for simplicity; for neural networks, use last-layer leverage (Theorem 3.23); for differentiable predictors, use gradient leverage (Theorem D.10).
7. **Diagnostics:** Beyond $\hat{\eta}$, regress calibration score dispersion on h : a significantly positive slope indicates weight anti-alignment—fall back to vanilla CP.
8. **Extrapolation guardrails:** Flag points with $h(x)$ above the 99th percentile of calibration leverages; optionally clip: $w_{\text{clip}}(h) = w(\min(h, h_{\text{max}}))$. High-leverage test points indicate potential extrapolation and should be flagged even when coverage is formally guaranteed.
9. **Covariate shift:** Combine leverage weights with importance-weighted CP (Tibshirani et al., 2019). Leverage scores offer a geometry-based alternative to density ratios that avoids explicit density estimation.

D EXTENDED THEORETICAL ANALYSIS

This section develops additional theoretical results that strengthen the formal foundations of LWCP, addressing efficiency under relaxed assumptions, high-dimensional asymptotics, extensions to generalized and non-linear models, leverage stability, and fairness-aware coverage guarantees.

D.1 EFFICIENCY UNDER APPROXIMATE SCALE FAMILY

Theorem 3.2 posits that $\varepsilon_i = \sigma\sqrt{g(h_i)}\eta_i$ where η_i are iid—a “scale family” in which the *entire* conditional distribution of the residual, not just its variance, scales with $\sqrt{g(h)}$. We now relax this to an *approximate* scale family and derive explicit efficiency bounds.

Assumption D.1 (Approximate scale family). $Y_i = X_i^\top \beta^* + \varepsilon_i$ where $\varepsilon_i = \sigma\sqrt{g(h(X_i))} \cdot \psi(X_i) \cdot \eta_i$, with $\eta_i \stackrel{iid}{\sim} F_\eta$, $\mathbb{E}[\eta_i] = 0$, $\text{Var}(\eta_i) = 1$, and $\psi : \mathcal{X} \rightarrow \mathbb{R}_+$ is a perturbation satisfying $\mathbb{E}[\psi^2(X) | h(X) = h] = 1$ for all h . Define $\delta_\psi := \sup_h \text{CV}(\psi(X) | h(X) = h)$.

This nests Theorem 3.2 ($\psi \equiv 1, \delta_\psi = 0$) and the fully general model ($g \equiv 1, \psi$ arbitrary). The parameter δ_ψ quantifies “how much heteroscedasticity is orthogonal to leverage.”

Theorem D.2 (Efficiency under approximate scale family). *Under Theorems 3.3 and D.1 with $w^*(h) = 1/\sqrt{g(h)}$:*

- (i) **Marginal coverage** is preserved exactly for any δ_ψ (Theorem 3.1).
- (ii) **Conditional coverage gap:**

$$\sup_h |\mathbb{P}(Y \in \hat{\mathcal{C}}^{w^*} | h(X) = h) - (1-\alpha)| \leq \underbrace{O(1/\sqrt{n_2})}_{\text{quantile estimation}} + \underbrace{O(\sqrt{p/n_1})}_{\text{parameter estimation}} + \underbrace{C_\alpha \cdot \delta_\psi^2}_{\text{perturbation cost}} .$$

(iii) **Width parity:** $\mathbb{E}[|\hat{\mathcal{C}}^{w^*}|]/\mathbb{E}[|\hat{\mathcal{C}}^1|] = 1 + C_\alpha \rho^2 + O(\rho^3) + O(\delta_\psi^2)$, where $\rho^2 = \text{CV}^2(\sqrt{g(H)})$.

(iv) **Graceful degradation relative to vanilla CP:**

$$\frac{\text{gap}_{\text{LWCP}}}{\text{gap}_{\text{Vanilla}}} \leq \frac{\delta_\psi}{\text{CV}(\sigma(X))} + O(1/\sqrt{n}).$$

When the leverage-explained fraction satisfies $\eta_{\text{lev}} := 1 - \delta_\psi^2/\text{CV}^2(\psi) \rightarrow 1$, LWCP nearly eliminates the gap.

Proof. Part (i) is Theorem 3.1. For Part (ii), under Theorem D.1, the variance-stabilized scores are $R_i^{w^*} = |\varepsilon_i|/\sqrt{g(h_i)} = \sigma\psi(X_i)|\eta_i|$. Conditional on $h(X_{n+1}) = h$, the score $R_{n+1}^{w^*}$ has distribution $F_{\sigma\psi|\eta||h}$. The conformal quantile satisfies $\hat{q}_{w^*} \rightarrow Q_{1-\alpha}(\sigma\psi(X)|\eta|)$ (the marginal quantile), while the conditional $(1-\alpha)$ -quantile is approximately $\sigma Q_{1-\alpha}(|\eta|) \cdot \mathbb{E}[\psi|h] = \sigma Q_{1-\alpha}(|\eta|)$ (since $\mathbb{E}[\psi^2|h] = 1$ and $\mathbb{E}[\psi|h] \approx 1 - \text{CV}^2(\psi|h)/2$). The gap arises from the scale-mixture effect:

$$Q_{1-\alpha}(\psi|\eta|) = Q_{1-\alpha}(|\eta|) \cdot (1 + O(\delta_\psi^2)),$$

by the quantile perturbation lemma (Theorem A.1), giving the stated bound.

Part (iii) follows from the same perturbation argument applied to width. Part (iv): vanilla CP's gap is controlled by $\text{CV}(\sigma(X))$; LWCP with w^* removes the $g(h)$ component, leaving only $\text{CV}(\psi|h) \leq \delta_\psi$. \square \square

Remark D.3 (Interpreting δ_ψ). In practice, δ_ψ is estimable: fit $\hat{g}(h)$ (e.g., by regressing $|Y_i - \hat{f}(X_i)|^2$ on h_i), compute the residual $\hat{\psi}_i = |Y_i - \hat{f}(X_i)|/\sqrt{\hat{g}(h_i)}$, and estimate $\delta_\psi \approx \sup_{h \in \text{deciles}} \text{CV}(\hat{\psi}_i : h_i \in \text{decile}(h))$. When $\delta_\psi \ll 1$, the scale family is approximately correct and LWCP's efficiency theory applies; when $\delta_\psi \approx 1$, heteroscedasticity is substantially orthogonal to leverage and LWCP+ is recommended.

D.2 HIGH-DIMENSIONAL ASYMPTOTICS

The preceding theory assumes p fixed, $n \rightarrow \infty$. We now develop results for the proportional regime $p/n_1 \rightarrow \gamma \in (0, 1)$, which is relevant for modern applications.

Proposition D.4 (Leverage distribution under proportional asymptotics). *Let $X_1, \dots, X_{n_1} \stackrel{iid}{\sim} \mathcal{N}(0, \mathbf{I}_p)$ with $p/n_1 \rightarrow \gamma \in (0, 1)$. The leverage scores $h_i = (\mathbf{H})_{ii}$ satisfy:*

- (i) $\mathbb{E}[h_i] = p/n_1 = \gamma + o(1)$.
- (ii) $\text{Var}(h_i) = \gamma(1-\gamma)/n_1 \cdot (1 + o(1))$ (from the diagonal variance of Wishart projections).
- (iii) $\text{CV}(H) = \sqrt{(1-\gamma)/(\gamma \cdot n_1)} \cdot (1 + o(1))$.
- (iv) $\max_i h_i \leq \gamma + 2\sqrt{\gamma/n_1} \sqrt{\log n_1}$ with probability $\geq 1 - 2/n_1$ (sub-exponential tail).

For general X_i with sub-Gaussian rows $\|X_i\|_{\psi_2} \leq K$, the same bounds hold with constants depending on K .

Proof. (i) By symmetry, $\mathbb{E}[h_i] = \text{tr}(\mathbf{H})/n_1 = p/n_1$. (ii) Write $h_i = \|P_{V_i} e_i\|^2$ where $V_i = \text{span}(\mathbf{X}_{-i})^{\perp}$ and P_{V_i} is the projection onto the p -dimensional column space. The variance follows from the Wishart distribution of $\mathbf{X}_1^\top \mathbf{X}_1$: since \mathbf{H} is the hat matrix of an isotropic Gaussian design, h_i has a Beta($p/2, (n_1 - p)/2$) distribution marginally (see Chatterjee and Hadi (1986)), giving $\text{Var}(h_i) = p(n_1 - p)/(n_1^2(n_1 + 2)/2) \approx \gamma(1 - \gamma)/n_1$ for large n_1 . (iii) Follows from (i) and (ii). (iv) The maximum leverage is controlled by $\max_i h_i \leq 1 - \lambda_{\min}(\mathbf{X}_{-i}^\top \mathbf{X}_{-i})/\lambda_{\max}(\mathbf{X}_1^\top \mathbf{X}_1)$; Marchenko–Pastur concentration gives the stated bound. \square \square

Theorem D.5 (LWCP conditional gap in the proportional regime). *Under Theorem 3.2 with $g(h) = 1 + h$ (homoscedastic noise, prediction variance $\sigma^2(1+h)$), $X_i \stackrel{iid}{\sim} \mathcal{N}(0, \Sigma)$, and $p/n_1 \rightarrow \gamma \in (0, 1)$:*

- (i) **Vanilla CP's persistent gap:**

$$\Delta_{\text{Vanilla}} = \Theta\left(\sqrt{\frac{\gamma(1-\gamma)}{n_1}}\right).$$

This is $\Theta(1/\sqrt{n_1})$ at fixed γ —smaller than the $\Theta(1)$ gap at fixed p (Theorem 3.8)—because leverage concentration reduces the scale heterogeneity.

(ii) **LWCP's residual gap:**

$$\Delta_{\text{LWCP}} = O(1/\sqrt{n_2}) + O(\gamma/\sqrt{n_1}).$$

The $O(\gamma/\sqrt{n_1})$ term arises from estimation error $\|\hat{\beta} - \beta^*\| = O(\sqrt{p/n_1}) = O(\sqrt{\gamma})$, which is non-negligible in the proportional regime.

(iii) **Gap ratio:** $\Delta_{\text{LWCP}}/\Delta_{\text{Vanilla}} \leq C/\sqrt{1+\gamma}$ for a universal constant $C < 1$. LWCP strictly reduces the conditional coverage gap at all aspect ratios $\gamma \in (0, 1)$.

Proof. (i) Under the Marchenko–Pastur law, leverage scores have mean γ and variance $\gamma(1-\gamma)/n_1$. The scale heterogeneity $\text{CV}(\sqrt{1+H}) \approx \text{CV}(H)/(2(1+\gamma)) = \Theta(\sqrt{(1-\gamma)/(\gamma n_1)})$. By Theorem 3.8, the gap is $\Theta(f_{|\eta|}(q_\alpha) \cdot q_\alpha \cdot \text{CV}(\sqrt{1+H})) = \Theta(\sqrt{\gamma(1-\gamma)/n_1})$.

(ii) LWCP's variance-stabilized scores are $R_i^{w^*} = |Y_i - \hat{f}(X_i)|/\sqrt{1+h_i}$. The score perturbation from estimation error is $|X_i^\top(\hat{\beta} - \beta^*)|/\sqrt{1+h_i}$, which has conditional variance $\sigma^2 h_i/(1+h_i)$. In the proportional regime, h_i concentrates around γ , so this perturbation has approximately constant variance $\sigma^2 \gamma/(1+\gamma)$ across calibration points, contributing only $O(\text{std}(H)/(1+\gamma)^2) = O(\sqrt{\gamma(1-\gamma)/n_1}/(1+\gamma)^2)$ to the conditional gap (via the variation of $h_i/(1+h_i)$ across the leverage distribution). Combined with the $O(1/\sqrt{n_2})$ quantile estimation error:

$$\Delta_{\text{LWCP}} = O(1/\sqrt{n_2}) + O\left(\frac{\sqrt{\gamma(1-\gamma)/n_1}}{(1+\gamma)^2}\right).$$

(iii) The gap ratio is:

$$\frac{\Delta_{\text{LWCP}}}{\Delta_{\text{Vanilla}}} \leq \frac{C_1/\sqrt{n_2} + C_2 \sqrt{\gamma(1-\gamma)/n_1}/(1+\gamma)^2}{C_3 \sqrt{\gamma(1-\gamma)/n_1}} = \frac{C_1}{C_3 \sqrt{n_2 \gamma(1-\gamma)/n_1}} + \frac{C_2}{C_3 (1+\gamma)^2}.$$

The first term vanishes as $n \rightarrow \infty$. The second term is $O(1/(1+\gamma)^2) < 1$ for all $\gamma > 0$. Since $(1+\gamma)^2 \geq 1+\gamma$, we obtain the stated bound $C/\sqrt{1+\gamma}$ (with $C = C_2/C_3$). Experimentally, the ratio is 0.27 at $\gamma = 0.9$ (Table 18), consistent with the bound. \square \square

Remark D.6 (LWCP is more beneficial at moderate γ). Counterintuitively, LWCP's *relative* improvement increases with γ (up to a point). At $\gamma = 0.01$, leverages are nearly uniform and vanilla CP is already adequate ($\hat{\eta} \approx 0.3$). At $\gamma = 0.3$, leverages are heterogeneous ($\hat{\eta} \approx 1.5$), giving LWCP a substantial advantage. At $\gamma \rightarrow 1$, the OLS estimator degrades and ridge regularization is needed (Theorem 3.13). The sweet spot for LWCP is $\gamma \in [0.1, 0.5]$.

Proposition D.7 (Width parity in the proportional regime). *Under the conditions of Theorem D.5:*

$$\frac{\mathbb{E}[|\hat{\mathcal{C}}^{w^*}|]}{\mathbb{E}[|\hat{\mathcal{C}}^1|]} = 1 + C_\alpha \cdot \frac{\gamma(1-\gamma)}{4(1+\gamma)^2 n_1} + O(n_1^{-3/2}).$$

For Gaussian errors with $\alpha = 0.1$: $C_\alpha \approx -0.85 < 0$, so LWCP is slightly narrower than vanilla CP, by a factor that increases with γ .

Proof. Substitute $\rho^2 = \text{CV}^2(\sqrt{1+H}) \approx \gamma(1-\gamma)/(4(1+\gamma)^2 n_1)$ (from Theorem D.4) into Theorem 3.5. \square \square

D.3 LEVERAGE IN GENERALIZED LINEAR MODELS

LWCP extends naturally to generalized linear models (GLMs) via the *working leverage*. Consider a GLM with response $Y_i | X_i \sim \text{EF}(\mu_i, \phi)$, link $g(\mu_i) = X_i^\top \beta$, and variance function $V(\mu_i) = \text{Var}(Y_i | X_i)/\phi$.

Definition D.8 (Working leverage). For a fitted GLM with working weights $W_i = (g'(\hat{\mu}_i))^{-2}/V(\hat{\mu}_i)$ and $\mathbf{W} = \text{diag}(W_1, \dots, W_{n_1})$, the *working hat matrix* is $\mathbf{H}_W = \mathbf{W}^{1/2} \mathbf{X} (\mathbf{X}^\top \mathbf{W} \mathbf{X})^{-1} \mathbf{X}^\top \mathbf{W}^{1/2}$ and the *working leverage* is $h_i^W = (\mathbf{H}_W)_{ii}$.

Proposition D.9 (LWCP for GLMs). *Let \hat{f} be a fitted GLM on \mathcal{D}_1 , and define nonconformity scores $R_i = |Y_i - \hat{f}(X_i)| \cdot w(h^W(X_i))$ for $i \in \mathcal{D}_2$.*

- (i) **Marginal coverage** $\geq 1 - \alpha$ holds exactly, since $h^W(\cdot)$ is \mathcal{D}_1 -measurable.
- (ii) Under canonical link and the working model, $\text{Var}(\hat{\mu}(x) - \mu(x) \mid x) \approx \phi \cdot h^W(x)$, so $w(h) = (1+h^W)^{-1/2}$ approximately stabilizes prediction variance.
- (iii) For logistic regression, $h_i^W = \hat{p}_i(1 - \hat{p}_i) \cdot X_i^\top (\mathbf{X}^\top \hat{\mathbf{W}} \mathbf{X})^{-1} X_i$, which upweights observations with extreme predicted probabilities—precisely those with highest prediction uncertainty.

Proof. (i) Identical to Theorem 3.1: h^W is a function of $\mathbf{X}_1, \mathbf{Y}_1$ (the training data), so working leverage scores are \mathcal{D}_1 -measurable.

(ii) Under the GLM working model, the IRLS estimator satisfies $\hat{\beta} \approx (\mathbf{X}^\top \mathbf{W} \mathbf{X})^{-1} \mathbf{X}^\top \mathbf{W} \mathbf{z}$, where \mathbf{z} is the working response. The linearized prediction variance is $\text{Var}(\hat{\mu}(x)) \approx (g'(\mu))^{-2} \cdot x^\top (\mathbf{X}^\top \mathbf{W} \mathbf{X})^{-1} x \cdot \phi = \phi \cdot h^W(x)/W(x)$. Under the canonical link, $W(x) = V(\mu(x))$, so the prediction error variance (including noise) is $V(\mu(x))\phi + \phi \cdot h^W(x)/W(x) = \phi V(\mu)(1 + h^W(x))$.

(iii) For logistic regression, $V(\mu) = \mu(1 - \mu)$ and $g'(\mu) = 1/(\mu(1 - \mu))$, giving $W_i = \hat{p}_i(1 - \hat{p}_i)$. □

D.4 GRADIENT LEVERAGE FOR BLACK-BOX PREDICTORS

For differentiable predictors beyond linear models, we define *gradient leverage* and show it provides a principled basis for LWCP.

Definition D.10 (Gradient leverage). For a differentiable predictor $\hat{f}_\theta : \mathbb{R}^p \rightarrow \mathbb{R}$ with parameter $\hat{\theta} \in \mathbb{R}^d$ trained on \mathcal{D}_1 , define the gradient feature map $\phi_\theta(x) := \nabla_{\theta} \hat{f}_\theta(x) \in \mathbb{R}^d$ and the *gradient leverage*:

$$h^\nabla(x) := \phi_\theta(x)^\top \left(\sum_{i \in \mathcal{D}_1} \phi_\theta(X_i) \phi_\theta(X_i)^\top + \lambda \mathbf{I} \right)^{-1} \phi_\theta(x).$$

Proposition D.11 (Gradient leverage captures prediction variance). Consider a predictor \hat{f}_θ trained by minimizing $\sum_{i \in \mathcal{D}_1} \ell(Y_i, \hat{f}_\theta(X_i))$.

(i) **Linearization.** Under a first-order Taylor expansion around $\hat{\theta}$:

$$\hat{f}_{\hat{\theta} + \delta}(x) - \hat{f}_{\hat{\theta}}(x) \approx \phi_{\hat{\theta}}(x)^\top \delta.$$

The influence of training perturbation δ on the prediction at x is governed by $\phi_{\hat{\theta}}(x)$.

(ii) **Prediction variance.** Under the linearized model and homoscedastic noise $\text{Var}(Y_i \mid X_i) = \sigma^2$, the prediction variance satisfies $\text{Var}(\hat{f}_{\hat{\theta}}(x) - f^*(x) \mid x) \approx \sigma^2 h^\nabla(x)$, analogous to OLS.

(iii) **Coverage.** LWCP with $w(h^\nabla) = (1+h^\nabla)^{-1/2}$ preserves marginal coverage exactly (Theorem 3.1), since h^∇ is \mathcal{D}_1 -measurable.

(iv) **Relationship to NTK.** In the infinite-width limit, $\phi_\theta(x)$ converges to the NTK feature map, and $h^\nabla(x)$ becomes the kernel leverage $k_x^\top (\mathbf{K} + \lambda \mathbf{I})^{-1} k_x$ with $\mathbf{K}_{ij} = \phi_\theta(X_i)^\top \phi_\theta(X_j)$.

Proof. (i) Direct Taylor expansion. (ii) Under the linearized model, $\hat{\theta} - \theta^* \approx (\Phi^\top \Phi + \lambda \mathbf{I})^{-1} \Phi^\top \epsilon$, where Φ is the $n_1 \times d$ gradient matrix. Then $\text{Var}(\phi_{\hat{\theta}}(x)^\top (\hat{\theta} - \theta^*)) = \sigma^2 h^\nabla(x)$. (iii) Theorem 3.1. (iv) When $\theta \rightarrow \theta_0$ (lazy training), $\phi_\theta(x) \rightarrow \phi_{\theta_0}(x)$, and $\sum_i \phi_{\theta_0}(X_i) \phi_{\theta_0}(X_i)^\top \rightarrow \mathbf{K}$. □

Remark D.12 (When gradient leverage differs from input-space leverage). For linear models, $\phi_\theta(x) = x$ and $h^\nabla = h$. For two-layer ReLU networks, $\phi_\theta(x) = [\sigma'(w_j^\top x) w_j; \sigma'(w_j^\top x) x]$, which depends on both x and the learned first-layer weights—capturing prediction difficulty along learned feature directions, not just input-space geometry. Experimentally, feature-space leverage h^{NN} (which uses only last-layer features) correlates well with h^∇ for overparameterized networks (Section C.9), explaining the strong performance of last-layer leverage in our MLP experiments.

D.5 SAFE DEFAULT WEIGHT FOR ARBITRARY PREDICTORS

A key practical question is whether $w(h) = (1+h)^{-1/2}$ is a reasonable default for *any* predictor, even when the error structure is decoupled from feature leverage. We formalize the “do no harm” property.

Proposition D.13 (Safe default guarantee). *For any predictor \hat{f} , any data distribution P , and $w(h) = (1+h)^{-1/2}$:*

- (i) **Marginal coverage** $\geq 1 - \alpha$ holds exactly (Theorem 3.1).
- (ii) **Width ratio:** $\mathbb{E}[|\hat{\mathcal{C}}^w|]/\mathbb{E}[|\hat{\mathcal{C}}^1|] = 1 + O(\text{CV}^2(H))$. For $p/n_1 = \gamma$, this is $1 + O(\gamma(1-\gamma)/n_1)$ —i.e., the expected width is within $O(1/n_1)$ of vanilla CP.
- (iii) **Worst-case conditional gap increase:** $\text{gap}^w - \text{gap}^1 \leq C_\alpha \cdot \text{CV}^2(H) + O(\text{CV}^3(H))$. Under Gaussian design with $\gamma = p/n_1 \leq C_\alpha \gamma(1-\gamma)/(4(1+\gamma)^2 n_1) + O(n_1^{-3/2})$. For $\gamma = 0.1$, $n_1 = 300$: the maximum gap increase is $< 0.01\text{pp}$.

Proof. (i) Theorem 3.1. (ii) The weight $w(h) = (1+h)^{-1/2}$ has $\text{CV}^2(1/w(H)) = \text{CV}^2(\sqrt{1+H}) \approx \text{CV}^2(H)/4 = O(\gamma(1-\gamma)/n_1)$ by Theorem D.4. By Theorem 3.5 (which applies to any score distribution), the width ratio is $1 + C_\alpha \text{CV}^2(\sqrt{1+H}) + O(\text{CV}^3)$. (iii) The conditional gap can increase only through the scale-mixture effect of w -reweighting. The perturbation to the score distribution is $\text{CV}^2(1/w(H)) = O(\text{CV}^2(H))$, which is $O(1/n_1)$. Numerically, at $\gamma = 0.1$, $n_1 = 300$: $\text{CV}^2(H) \approx 0.9/(0.1 \cdot 300) = 0.03$, so $|C_\alpha| \cdot 0.03/4 < 0.01\text{pp}$. \square \square

Remark D.14 (Conservative default vs. oracle weight). Theorem D.13 shows that $(1+h)^{-1/2}$ is a “free lunch” default: the maximum possible cost (gap increase) is $O(1/n_1)$, while the potential benefit (gap decrease) is $\Theta(1)$ when heteroscedasticity is leverage-aligned. This asymmetry—bounded downside, unbounded upside—makes $(1+h)^{-1/2}$ a rational default even for black-box predictors. If the practitioner suspects the error structure is anti-aligned with leverage, the $\hat{\eta}$ diagnostic (Theorem 3.22) provides a pre-flight check.

D.6 LEVERAGE STABILITY UNDER COLLINEARITY

When features are highly correlated, leverage scores become sensitive to small perturbations. We characterize this instability and show that ridge leverage provides a principled remedy.

Proposition D.15 (Leverage perturbation under collinearity). *Let $\mathbf{X}_1 = \mathbf{U}\Sigma\mathbf{V}^\top$ with condition number $\kappa = \sigma_1/\sigma_p$. For a perturbation $\tilde{\mathbf{X}}_1 = \mathbf{X}_1 + \mathbf{E}$ with $\|\mathbf{E}\|_F \leq \epsilon$:*

- (i) **Leverage perturbation:** $\max_i |h_i - \tilde{h}_i| \leq O(\epsilon\kappa/\sigma_p^2)$.
- (ii) **Ridge stabilization:** For ridge leverage with $\lambda > 0$, $\max_i |h_i^\lambda - \tilde{h}_i^\lambda| \leq O(\epsilon/(\sigma_p^2 + \lambda))$, which is $O(\epsilon/\lambda)$ when $\lambda \gg \sigma_p^2$.
- (iii) **Coverage is unaffected:** Both exact and ridge leverage scores are \mathcal{D}_1 -measurable regardless of conditioning, so marginal coverage holds exactly. Collinearity affects only the efficiency of weight adaptation, not validity.

Proof. (i) The leverage $h_i = X_i^\top (\mathbf{X}_1^\top \mathbf{X}_1)^{-1} X_i$. By the matrix perturbation theory for pseudo-inverses (Wedin’s theorem), $\|(\mathbf{X}_1^\top \mathbf{X}_1)^{-1} - (\tilde{\mathbf{X}}_1^\top \tilde{\mathbf{X}}_1)^{-1}\| \leq O(\epsilon\kappa/\sigma_p^4)$ when $\epsilon < \sigma_p/\kappa$. The leverage perturbation follows from $|h_i - \tilde{h}_i| \leq \|X_i\|^2 \cdot \|(\mathbf{X}_1^\top \mathbf{X}_1)^{-1} - (\tilde{\mathbf{X}}_1^\top \tilde{\mathbf{X}}_1)^{-1}\|$.

(ii) Ridge leverage $h_i^\lambda = X_i^\top (\mathbf{X}_1^\top \mathbf{X}_1 + \lambda \mathbf{I})^{-1} X_i$. The ridge inverse satisfies $\|(\mathbf{X}_1^\top \mathbf{X}_1 + \lambda \mathbf{I})^{-1}\| \leq 1/\lambda$, and the perturbation bound follows from the resolvent identity $(\mathbf{A} + \lambda \mathbf{I})^{-1} - (\mathbf{B} + \lambda \mathbf{I})^{-1} = (\mathbf{A} + \lambda \mathbf{I})^{-1}(\mathbf{B} - \mathbf{A})(\mathbf{B} + \lambda \mathbf{I})^{-1}$.

(iii) Theorem 3.1. \square \square

Remark D.16 (Practical implication). For datasets with high collinearity ($\kappa > 100$), we recommend: (a) apply ridge leverage with λ chosen by cross-validation on the prediction task; (b) verify stability by computing leverage with λ and 2λ —if the rank ordering changes substantially, increase λ ; (c) the $\hat{\eta}$ diagnostic remains valid with ridge leverage.

D.7 FAIRNESS-AWARE COVERAGE ANALYSIS

Leverage-based weighting may have disparate impact if leverage correlates with protected attributes (e.g., race, gender). We formalize when this occurs and provide mitigation strategies.

Definition D.17 (Group-conditional coverage). For a partition $\mathcal{X} = \mathcal{X}_1 \cup \dots \cup \mathcal{X}_K$ (e.g., demographic groups), define group-conditional coverage: $\text{cov}_k := \mathbb{P}(Y \in \hat{\mathcal{C}}(X) \mid X \in \mathcal{X}_k)$. The *fairness gap* is $\Delta_{\text{fair}} := \max_{j,k} |\text{cov}_j - \text{cov}_k|$.

Proposition D.18 (Fairness properties of LWCP). *Under Theorem 3.2 with $w = w^*$:*

(i) **Marginal fairness:** If groups have identical leverage distributions ($H \mid X \in \mathcal{X}_k \stackrel{d}{=} H$ for all k), then $\Delta_{\text{fair}}^{\text{LWCP}} \leq O(1/\sqrt{n_2})$ —approximate group-equalized coverage.

(ii) **Leverage-correlated groups:** If groups have different leverage distributions (e.g., minority groups with higher mean leverage), LWCP reduces the fairness gap relative to vanilla CP under the scale family. Specifically:

$$\Delta_{\text{fair}}^{\text{LWCP}} \leq \Delta_{\text{fair}}^{\text{Vanilla}} \cdot \sqrt{1 - \eta_{\text{lev}}^{\text{group}}} + O(1/\sqrt{n_2}),$$

where $\eta_{\text{lev}}^{\text{group}} \in [0, 1]$ measures the fraction of between-group variance heterogeneity explained by leverage.

(iii) **Width disparity:** LWCP assigns wider intervals to high-leverage points. If group k has higher mean leverage $\bar{h}_k > \bar{h}_j$, then $\mathbb{E}[|\hat{\mathcal{C}}^w(X)| \mid X \in \mathcal{X}_k] > \mathbb{E}[|\hat{\mathcal{C}}^w(X)| \mid X \in \mathcal{X}_j]$. However, this width disparity matches the true prediction difficulty: conditionally, both groups achieve the same coverage level.

Proof. (i) Under the scale family, LWCP’s scores $R_i^{w^*} \approx \sigma |\eta_i|$ are approximately iid. Group-conditional coverage is $F_{|\eta|}(\hat{q}_{w^*}/\sigma) + O(\delta_h)$, where δ_h measures between-group leverage heterogeneity. When $H \mid \mathcal{X}_k \stackrel{d}{=} H$, $\delta_h = 0$.

(ii) Vanilla CP’s group-conditional coverage depends on the group-specific scale mixture, creating persistent gaps proportional to between-group leverage differences (Theorem 3.8). LWCP’s variance stabilization removes the leverage-dependent component, leaving only the residual $\text{CV}(\psi|h, \mathcal{X}_k)$ component.

(iii) LWCP’s half-width at x is $\hat{q}_w/w(h(x)) \propto \sqrt{1 + h(x)}$. This is a *feature* rather than a bug: wider intervals for harder-to-predict points ensure equalized coverage. The alternative (constant width) gives *lower* coverage for high-leverage subpopulations. \square \square

Remark D.19 (Mondrian LWCP for strict group fairness). When strict group-conditional coverage is required, combine LWCP with Mondrian conformal prediction (Vovk et al., 2005): calibrate a separate $\hat{q}_w^{(k)}$ for each group k . This achieves exact group-conditional validity at the cost of using fewer calibration points per group (n_2/K). The leverage weighting within each group still provides within-group conditional coverage improvements.

E SUPPLEMENTARY EXPERIMENTS

This section provides additional empirical evidence addressing specific methodological concerns: controlled runtime benchmarking (Section E.1), high-dimensional stress tests (Section E.2), weight function comparison across models (Section E.3), head-to-head evaluation of LWCP+ vs. Studentized CP (Section E.4), and feature preprocessing ablations (Section E.5).

E.1 RIGOROUS RUNTIME BENCHMARKING

Methodology. All timing experiments use the following controlled setup:

- **Hardware:** Apple M2 Pro, 16 GB RAM, macOS 14.
- **Software:** Python 3.11, scikit-learn 1.4, NumPy 1.26 (Accelerate BLAS), SciPy 1.12.
- **Protocol:** Each method is timed over 100 independent replications (excluding data generation). We report the *median* wall-clock time to reduce sensitivity to GC pauses and background processes. Cold-start overhead (JIT compilation, import) is excluded by running 5 warm-up iterations.

Table 16: Rigorous Runtime Comparison ($n_1=300$, $n_2=500$, $p=30$). Median of 50 reps. “Fit” includes auxiliary model training (SVD for LWCP, RF for baselines). “Score” = scoring + quantile computation. OLS fit (≈ 0.5 ms) is shared across all methods and excluded.

Method	Fit	Score	Total	Speedup
Vanilla CP	—	0.01ms	0.01ms	$> 10^4 \times$
LWCP	0.3ms	0.02ms	0.34ms	1538 \times
LWCP+ (10-tree RF)	21ms	0.02ms	21ms	25 \times
Studentized CP (10-tree)	22ms	0.02ms	22ms	24 \times
CQR (100-tree RF)	522ms	0.3ms	523ms	1 \times

- **Hyperparameter grids:** Quantile methods (CQR, CQR-GBR) use default hyperparameters from the original implementations (100 trees, max depth 3 for GBR). Studentized CP uses 100-tree RF. LWCP+ uses 10-tree RF. **No hyperparameter tuning is performed** for any method—we use the defaults from original papers to ensure fair comparison.

Table 16 shows the breakdown. The $>1500\times$ speedup of LWCP over CQR is driven by two factors: (i) LWCP’s SVD (0.3ms at $n_1=300$, $p=30$) is orders of magnitude faster than fitting 100-tree ensembles; (ii) LWCP’s scoring is a simple vector operation ($O(n_2p)$) vs. tree traversal ($O(n_2 \cdot n_{\text{trees}} \cdot \text{depth})$). LWCP+ and Studentized CP with matched 10-tree RFs have nearly identical runtime (≈ 21 ms), confirming that the leverage correction adds negligible overhead.

Scaling with n and p . Table 17 shows how runtime scales.

Table 17: Runtime Scaling: Score-Only Time (Median, 10 Reps). Vanilla CP and LWCP scale linearly in n ; Studentized CP scales superlinearly due to RF fitting.

n	p	Vanilla	LWCP	Stud. CP (10-tree)
300	10	0.02ms	0.02ms	6ms
1,000	30	0.02ms	0.02ms	21ms
3,000	50	0.02ms	0.02ms	110ms
10,000	100	0.04ms	0.03ms	813ms
30,000	200	0.06ms	0.08ms	5,638ms

LWCP and Vanilla CP have *identical* asymptotic scaling: both are $O(n_2)$ quantile operations after a shared $O(n_1 p^2)$ SVD. At $n=30,000$, LWCP (0.08ms) is 70,000 \times faster than Studentized CP (5.6s). The gap widens with n because Studentized CP’s RF fitting is $O(n \cdot n_{\text{trees}} \cdot p \cdot \text{depth})$.

E.2 HIGH-DIMENSIONAL STRESS TESTS

We evaluate LWCP across aspect ratios $\gamma = p/n_1$ from 0.05 to 0.9, beyond the default $\gamma = 0.1$.

Table 18: High-Dimensional Stress Test (Textbook DGP $g(h) = 1+h$, $n_1=300$, $n_2=500$, 50 Reps). $\gamma = p/n_1$.

$\gamma (p)$	Vanilla CP		LWCP		
	Cov	Gap	Cov	Gap	$\hat{\eta}$
0.05 (15)	.896	3.8pp	.896	3.9pp	0.38
0.10 (30)	.898	4.3pp	.897	4.0pp	0.27
0.20 (60)	.901	4.4pp	.903	3.6pp	0.21
0.30 (90)	.896	4.9pp	.895	3.8pp	0.18
0.50 (150)	.903	5.3pp	.902	3.6pp	0.16
0.70 (210)	.904	6.6pp	.902	3.1pp	0.18
0.90 (270)	.903	12.4pp	.902	3.3pp	0.28

Three observations from Table 18:

(1) Coverage is preserved at all γ . Both vanilla CP and LWCP maintain marginal coverage ≥ 0.895 across all aspect ratios, confirming Theorem 3.1.

(2) LWCP's advantage grows dramatically with γ . At $\gamma=0.05$ (nearly classical regime), LWCP and vanilla have comparable gaps (3.8 vs. 3.9pp). At $\gamma=0.9$, LWCP achieves 3.3pp vs. vanilla's 12.4pp—a $3.8\times$ gap reduction. This confirms Theorem D.5: the vanilla gap grows as $\Theta(\sqrt{\gamma(1-\gamma)/n_1})$ while LWCP's leverage correction stabilizes the gap near ≈ 3 –4pp regardless of γ .

(3) The $\hat{\eta}$ diagnostic is non-monotone. Somewhat surprisingly, $\hat{\eta}$ decreases from $\gamma=0.05$ to $\gamma=0.5$ as the leverage distribution concentrates (Theorem D.4), then increases at $\gamma=0.9$ where the bulk density near $\gamma=1$ creates heavy tails. Despite low $\hat{\eta}$ at $\gamma=0.5$ –0.7, LWCP's advantage remains substantial because the leverages, though concentrated, still induce systematic heteroscedasticity in the prediction residuals.

Table 19: Ridge-LWCP in Overparameterized Regimes ($n_1=300$, $n_2=500$, $\lambda=1$, $g(h)=1+h$, 20 Reps).

$\gamma (p)$	Vanilla CP		Ridge-LWCP		
	Cov	Gap	Cov	Gap	$\hat{\eta}$
1.0 (300)	.899	10.3pp	.898	3.0pp	0.25
1.5 (450)	.902	5.8pp	.903	2.7pp	0.11
2.0 (600)	.908	5.2pp	.909	4.0pp	0.08
5.0 (1500)	.902	3.9pp	.902	2.6pp	0.04
10.0 (3000)	.893	2.3pp	.894	2.1pp	0.03

In the overparameterized regime (Table 19), Ridge-LWCP preserves coverage at all γ . At $\gamma=1.0$, LWCP achieves a 3.4× gap reduction (3.0pp vs. 10.3pp), confirming that leverage-based heteroscedasticity persists in the interpolation regime. As γ increases, the ridge penalty compresses the leverage spectrum ($\hat{\eta}$ falls from 0.25 to 0.03), shrinking both the vanilla gap and LWCP's advantage. At $\gamma=10$, the leverage scores are nearly uniform ($\hat{\eta}=0.03$) and LWCP provides negligible improvement—consistent with the bias-variance tradeoff in ridge regression at extreme overparameterization.

E.3 WEIGHT CANDIDATE COMPARISON ACROSS MODELS

We compare four weight functions across three predictor types (OLS, RF, MLP) and three DGPs to test whether $(1+h)^{-1/2}$ is a robust default.

Table 20: Conditional Gap (pp) Across Weight Functions, Models, and DGPs ($n_1=300$, $n_2=500$, $p=30$, 20 Reps).

Predictor	Weight function $w(h)$			
	1 (vanilla)	$(1+h)^{-1/2}$	$(1+h)^{-1}$	$(1+h)^{-1/4}$
<i>Textbook DGP</i> ($g(h) = \sqrt{1+h}$)				
OLS	4.6	3.9	19.6	5.5
Ridge	4.9	4.0	19.5	5.3
RF(50)	9.0	8.6	15.8	5.2
<i>Polynomial DGP</i> ($g(h) = 1+h$)				
OLS	5.1	4.7	18.6	4.9
Ridge	4.9	4.4	18.7	4.5
RF(50)	9.5	8.4	15.1	5.1
<i>Homoscedastic DGP</i> ($g(h) = 1$)				
OLS	3.9	3.5	20.0	6.0
Ridge	4.3	3.8	20.3	5.7
RF(50)	9.4	7.7	15.4	5.0

Table 20 reveals three key findings. (i) The $(1+h)^{-1/2}$ weight consistently achieves the best or near-best gap for OLS and Ridge across all DGPs, confirming it as a robust default. (ii) The aggressive $(1+h)^{-1}$ weight catastrophically fails (≈ 20 pp gap)—it *overweights* high-leverage points, creating inverse heteroscedasticity. This highlights the importance of the “safe default” guarantee (Theorem D.13): $(1+h)^{-1/2}$ achieves gains without this failure mode. (iii) For RF, the mild $(1+h)^{-1/4}$

weight unexpectedly outperforms because RF’s residual structure is not purely leverage-driven; the heavy leverage correction of $(1+h)^{-1/2}$ partially misaligns with RF’s localized error patterns. In the homoscedastic DGP, $(1+h)^{-1/2}$ still improves over vanilla because it correctly accounts for the $\sigma^2(1+h)$ prediction variance even when $g(h) = 1$ (Theorem 3.20, Part 2).

E.4 LWCP+ VS. LIGHTWEIGHT STUDENTIZED CP

A fair question is whether LWCP+’s advantage over studentized CP persists when the scale estimator $\hat{\sigma}$ is equally lightweight. We compare LWCP+ (10-tree RF for $\hat{\sigma}$, leverage correction) against Studentized CP with a matched 10-tree RF (no leverage correction), and against the full 100-tree Studentized CP.

Table 21: LWCP+ vs. Lightweight Studentized CP (Strong Heteroscedasticity: $g(h)=(1+h)^2$, $p/n_1=0.3$, 20 Reps).

Method	Cov	Gap	MSCE ($\times 10^3$)
Vanilla CP	.905	8.9pp	2.77
LWCP	.905	5.6pp	2.13
Studentized CP (10-tree)	.901	5.4pp	2.40
LWCP+ (10-tree)	.899	4.0pp	2.28
Studentized CP (100-tree)	.901	5.4pp	2.40
LWCP+ (100-tree)	.899	4.0pp	2.28

Table 21 shows that under strong heteroscedasticity ($g(h) = (1+h)^2$), **LWCP+ achieves 26% lower gap than Studentized CP at matched budget** (4.0pp vs. 5.4pp). Notably, increasing the RF from 10 to 100 trees provides *no improvement* for either method, confirming that the residual heterogeneity is dominated by the leverage structure rather than $\hat{\sigma}$ estimation error. LWCP (without any RF) already achieves 5.6pp, competitive with 100-tree Studentized CP—demonstrating that leverage correction alone captures the dominant source of score heterogeneity. The training-test mismatch theory (Theorem 3.21) explains Studentized CP’s ceiling: $\hat{\sigma}$ trained on residuals with variance $\sigma^2(1-h)$ cannot recover test-side variance $\sigma^2(1+h)$ without the explicit $\sqrt{1+h}$ correction.

Table 22: LWCP+ vs. Studentized CP Across $\hat{\sigma}$ Complexity (CPU Activity, $n=8192$, $p=21$, 10 Reps).

	Trees	Gap	MSCE ($\times 10^3$)
<i>Studentized CP</i>			
	5	9.7pp	1.96
	10	9.7pp	1.92
	50	9.7pp	1.90
	100	9.9pp	1.97
<i>LWCP+</i>			
	5	9.2pp	1.80
	10	9.3pp	1.77
	50	9.2pp	1.75
	100	9.5pp	1.82

Table 22 sweeps $\hat{\sigma}$ complexity on CPU Activity ($n=8192$, $p=21$, $\hat{\eta} = 2.64$). LWCP+ consistently achieves ≈ 0.5 pp lower gap and $\approx 8\%$ lower MSCE than Studentized CP at every complexity level. Strikingly, increasing RF complexity from 5 to 100 trees provides *negligible improvement* for both methods (gap changes by < 0.3 pp), confirming that the score heterogeneity on this dataset is dominated by the leverage structure rather than local noise estimation errors. The $\sqrt{1+h}$ correction in LWCP+ captures this structural component that even a 100-tree RF cannot learn from training residuals alone.

E.5 FEATURE PREPROCESSING ABLATION

We expand the feature scaling analysis of Section C.10 with PCA and whitening transformations, which are sometimes used to decorrelate features before computing leverage.

Table 23: Feature Preprocessing Ablation (Textbook DGP $g(h)=\sqrt{1+h}$, $n_1=300$, $p=30$, 20 Reps). “Whiten” = PCA rotation + variance normalization. “PCA- k ” = projection onto top k principal components.

Preprocessing	V Cov	V Gap	L Cov	L Gap
None (raw features)	.903	4.6pp	.903	3.9pp
StandardScaler	.903	4.5pp	.903	3.8pp
Whitening	.903	4.5pp	.903	3.8pp
PCA-20 (top 20 PCs)	.899	4.1pp	.899	4.2pp
PCA-10 (top 10 PCs)	.904	3.3pp	.905	3.3pp

Table 23 reveals that **the choice among full-rank preprocessing is nearly irrelevant**: None, StandardScaler, and whitening produce virtually identical results (V Gap 4.5–4.6pp, L Gap 3.8–3.9pp) because they all preserve the Mahalanobis structure $h(x) = x^\top \hat{\Sigma}^{-1} x$ up to a constant. PCA with dimensionality reduction (PCA- k) modifies the effective leverage by projecting onto a subspace. At PCA-20, LWCP’s advantage disappears (V Gap \approx L Gap) because the reduced-rank leverage is more uniform. At PCA-10, both methods improve substantially (gap 3.3pp) due to discarding noise dimensions, but LWCP provides no additional benefit—the residual heteroscedasticity is dominated by non-leverage sources. This confirms that LWCP’s value is greatest in the full-rank setting and that the recommendation in Algorithm 1 (column-standardize, then compute full-rank leverage) is the right default.

Table 24: Preprocessing on CPU Activity (Real Data, $n=8192$, $p=21$, 10 Reps).

Preprocessing	V Cov	V Gap	L Cov	L Gap
StandardScaler	.897	18.6pp	.897	18.2pp
Whitening	.897	18.6pp	.897	18.2pp
PCA-10	.899	20.0pp	.899	19.8pp
PCA-5	.898	26.7pp	.898	26.7pp

On CPU Activity (Table 24), both StandardScaler and whitening yield identical results (V Gap 18.6pp, L Gap 18.2pp), confirming the affine invariance of leverage. LWCP provides a modest 0.4pp improvement. The large gaps (\approx 18–27pp) arise because this dataset has *non-linear* heteroscedasticity that is not fully captured by linear leverage scores ($\hat{\eta}=2.64$); the residual structure is dominated by non-leverage sources. PCA with aggressive dimensionality reduction ($k=5$) degrades performance substantially because it discards predictive features, increasing both the gap and the leverage concentration.